

*ANALYTICAL AND NUMERICAL STUDIES ON
FRP STRENGTHENED REINFORCED CONCRETE
COLUMNS UNDER TORSIONAL LOADING*

GOWLLA JYOTHSNA

CE14MTECH11001

A Dissertation Submitted to
Indian Institute of Technology Hyderabad
In Partial Fulfilment of the Requirements for
The Degree of Master of Technology



भारतीय प्रौद्योगिकी संस्थान हैदराबाद
Indian Institute of Technology Hyderabad

DEPARTMENT OF CIVIL ENGINEERING
INDIAN INSTITUTE OF TECHNOLOGY HYDERABAD

JUNE, 2016.

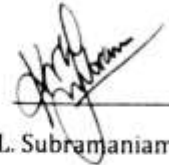
Declaration

I declare that this written submission represents my ideas in my own words, and where others' ideas or words have been included, I have adequately cited and referenced the original sources. I also declare that I have adhered to all principles of academic honesty and integrity and have not misrepresented or fabricated or falsified any idea/data/fact/source in my submission. I understand that any violation of the above will be a cause for disciplinary action by the Institute and can also evoke penal action from the sources that have thus not been properly cited, or from whom proper permission has not been taken when needed.


Gowlla Jyothsna
ce14mtech11001

Approval Sheet

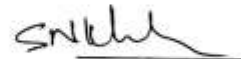
This thesis entitled "***Analytical and Numerical studies of FRP Strengthened Reinforced Concrete Columns under Torsional Loading***" by Gowlla Jyothsna is approved for the degree of Master of Technology from IIT Hyderabad.



Prof. K. V. L. Subramaniam
Examiner



Dr. Anil Agarwal
Examiner



Dr. Syed Nizamuddin Khaderi
Examiner



Dr. S. Suriya Prakash
Advisor

ABSTRACT

Bridges give the impression of being rather simple structural systems. Despite their structural simplicity, bridges in particular have not performed as expected under seismic attack. Under earthquake loading, bridge super structures will in general experience both rotational and translational motions. As a consequence, the supporting columns may be subjected to significant torsion, which is often ignored in typical design practice. Torsion results in brittle mode of failure which is undesirable and therefore, it is necessary to design it properly for avoiding brittle failures. Over the years, engineers have developed different methods and techniques in order to retrofit or strengthen the structures. The research carried till now on strengthening techniques of columns focuses mainly on those which are subjected to uniaxial eccentric loading under bending, shear and axial loads. However, till now, no previous study has focused on strengthening of reinforced concrete (RC) columns under torsional loading. The present study focuses on filling this knowledge gap. Nonlinear FE models are developed using commercial package ABAQUS and analysis were carried on to understand the behaviour of RC columns under torsional loading with and without FRP strengthening. Similarly, analysis is carried on in MATLAB by using Softened Membrane Model for Torsion with FRP (SMMT-FRP). The FE and analytical results gave a good agreement when validated with test data. After validation, behaviour of FRP strengthened RC Columns with under torsional loading is analysed. Analysis included various parametric studies like varying thickness of FRP laminate, number of layers,

alignment of FRP and increasing the level of applied axial load. Finally, interaction diagram between axial compression and torsional moment is also predicted.

CONTENTS

DECLARATION	<i>ERROR! BOOKMARK NOT DEFINED.</i>
APPROVAL SHEET	<i>ERROR! BOOKMARK NOT DEFINED.</i>
ABSTRACT	4
LIST OF FIGURES	9
LIST OF TABLES	11
<i>CHAPTER-1</i>	13
INTRODUCTION	13
1.1 GENERAL:	13
1.2 STRUCTURAL STRENGTHENING WITH FRP COMPOSITES:	16
1.2.1 Advantages of Composites:	17
1.3 NECESSITY FOR STRENGTHENING:	19
1.4 RESEARCH MOTIVATION:	20
1.5 OBJECTIVES AND SCOPE:	21
<i>CHAPTER-2</i>	25
LITERATURE REVIEW	25
2.1 BEHAVIOR OF RC COLUMNS UNDER TORSION:	25
2.2 BEHAVIOR OF RC BEAMS UNDER TORSION:	27
2.3 FRP STRENGTHENED BEAMS:	28
2.4 BEHAVIOR OF FRP STRENGTHENED RC COLUMNS:	29
<i>CHAPTER-3</i>	32
FINITE ELEMENT ANALYSIS	32
3.1 INTRODUCTION	32
3.2 ELEMENTS:	34
3.3 MATERIAL MODELS:	34
3.3.1 Concrete – Damage Plasticity Model:	34
3.3.2 Steel	37
3.3.3 FRP:	37
3.4 PROCEDURE – DYNAMIC EXPLICIT:	38

3.5 STEEL – CONCRETE INTERFACE:	38
3.6 LOAD AND BOUNDARY CONDITIONS:	39
3.7 MESHING	40
<i>CHAPTER-4</i>	42
SOFTENED MEMBRANE MODEL FOR TORSION WITH FRP	42
4.1 INTRODUCTION:	42
4.2 SOFTENED MEMBRANE MODEL FOR TORSION:	43
4.3 SOFTENED MEMBRANE MODEL FOR TORSION-FRP(SMMT-FRP)	44
4.3.1 Navier’s Principles Of Mechanics:	45
4.3.1.1 Stress equilibrium equations:	45
4.3.1.2 Strain compatibility equations:	47
4.3.2 Constitutive Laws Of Materials:	47
4.3.2.1 Constitutive relationship of concrete in compression:	47
4.3.2.1.1 Softening effect of concrete:	47
4.3.2.1.2 Strain gradient effect:	49
4.3.2.1.3 Confinement effect of FRP:	50
4.3.2.2 Constitutive relationship of concrete in tension:	53
4.3.2.3 Constitutive relationship of steel bars embedded in concrete:	54
4.3.2.3.1 Longitudinal steel reinforcement:	54
4.3.2.3.2 Transverse steel reinforcement:	54
4.3.2.4 Constitutive relationship of FRP:	55
4.3.2.5 Constitutive relationship of concrete in shear:	55
4.3.3 Additional Equations For Torsion:	55
4.3.3.1 Thickness of shear flow zone(T_D):	55
4.3.3.2 Area (A_0) and perimeter (P_0) of a shear flow:	57
4.3.3.3 Poisson’s effect:	58
4.3.4 Solution Algorithm For SMMT-FRP:	59
4.3.5 Nomenclature:	61
<i>CHAPTER - 5</i>	65
RESULTS AND DISCUSSION	65

PART-I	65
5.1 VALIDATION OF THE DEVELOPED MODEL (F.E.A):	65
5.2 EFFECT OF STRENGTHENING THE COLUMNS WITH FRP:	67
PART-II	70
5.3 VALIDATION OF THE DEVELOPED MODEL (MATLAB):	70
5.4 EFFECT OF STRENGTHENING THE COLUMNS WITH FRP:	71
5.5 PARAMETRIC STUDY:	72
5.5.1 Effect Of Thickness Of FRP Sheet:	72
5.5.2 Effect Of Multiple Layers Of FRP Sheets:	73
5.5.3 Effect Of FRP Sheet Alignment:	75
5.5.4 Effect Of Axial Compression:	76
5.5.4.1 Unstrengthened columns:	76
5.5.4.2 FRP strengthened columns:	77
5.5.5 Torsion-Axial Load Interaction Diagram:	80
<i>CHAPTER – 6</i>	85
6.1 CONCLUSIONS:	85
6.2 SCOPE FOR FUTURE STUDY:	86
6.3 REFERENCES:	86

LIST OF FIGURES

<i>Fig. No</i>	<i>Name of the figure</i>	<i>Pg.No</i>
1.1(a)	Outrigger bent	15
1.1(b)	Skewed bridge deck	15
1.1(c)	Variation in length of spalling zone with increase in torsion	20
3.1(a)	Cross section of the circular specimen	33
3.1(b)	Cross section of the square specimen	33
3.2(a)	C3D8R element	34
3.2(b)	S4R element	34
3.3.2	Coupon test results for steel used in circular columns	37
4.3.1(a)	R.C element subjected to torque and shear element to in plane shear flow	45
4.3.1(b)	FRP-RC membrane element subjected to in plane stresses under torsion	46
4.3.1.2(a)	Warped hyperboloid surface along 1 and 2 direction	49
4.3.1.2(b)	Strain gradient effect along principal direction	50
4.3.2 (a)	Compressive stress strain curve of concrete	51
4.3.2 (b)	Tensile stress strain curve of concrete	51
4.3.2 (c)	Stress strain behaviour of steel	51
4.3.2 (d)	Stress strain behaviour of FRP	52
4.3.3 (a)	Cross section of concrete strut	56
4.3.3 (b)	Strain distribution	56
4.3.4	Solution algorithm of SMMT-FRP	59
5.1 (a)	Torque-twist behaviour of circular column	65
5.1 (b)	Torque-twist behaviour of square column	65
5.1 (c)	Damage distribution in circular column	66
5.2 (a)	Torque-twist behaviour of circular column strengthened with FRP	67

5.2 (b)	Torque-twist behaviour of square column strengthened with FRP	67
5.2 (c)	Damage distribution of circular & square columns strengthened with FRP	68
5.3	Overall torque-twist behaviour of circular column	69
5.4	Torque-twist behaviour of column strengthened with and without FRP	70
5.5.1	Torque-twist behaviour of circular column by varying thickness of FRP	71
5.5.2 (a)	Torque-twist behaviour of 1mm FRP wrapped column by varying layers	73
5.5.2 (b)	Torque-twist behaviour of 2mm FRP wrapped column by varying layers	73
5.5.3	Torque-twist behaviour of column by varying alignment of FRP	74
5.5.4 (a)	Torque-twist behaviour of column under torsion and various axial loads	76
5.5.4 (b)	Torque-twist behaviour of FRP strengthened column under torsion and various axial loads	77
5.5.4 (c)	Torque-twist behaviour of columns with and without FRP under torsion and same axial loads.	78
5.5.5 (a)	Stress-strain curve for unconfined and FRP confined concrete	80
5.5.5 (b)	Axial compression-Torsional moment interaction diagram	82

LIST OF TABLES

<i>Table. No</i>	<i>Name of the table listed</i>	<i>Pg. No</i>
1	Specimen Details	23
2	Type and properties of FRP used	27

CHAPTER – 1

INTRODUCTION

CHAPTER-1

INTRODUCTION

1.1 GENERAL:

The damages observed after earthquakes has indicated that torsional oscillations are often the cause of distress in buildings and bridges. Reinforced concrete (RC) columns of skewed and curved bridges with unequal spans or column heights can be subjected to combined loading including axial, flexure, shear, and torsion loads during earthquakes. This combination of seismic loading can induce the complex flexural and shear failure of bridge columns. The presence of torsion significantly affects the inelastic flexural response of RC members under seismic loadings and results in brittle failure modes. In particular, torsional moments occur in RC structure elements (i) due to eccentric loads caused by traffic conditions in bridge box girders, (ii) when a spandrel beam meets at a corner without a column and (iii) in curved beams, staircases, and girders with horizontal projections. The addition of torsional moment is more likely in skewed and horizontally curved bridges, bridges with unequal spans or column heights and bridges with outrigger bents. Construction of bridges with these configurations is often unavoidable due to site constraints imposed by rivers, railroad tracks and other obstacles that do not necessarily cross a bridge perpendicular to its alignment. Accordingly, bridge members are often built in a skew or in a curved fashion to

accommodate such obstacles. Because, the responses of curved bridges under longitudinal and transverse motions are coupled, the columns can be subject to multidirectional deformation with torsion. This combination of seismic loading can have significant effects on the force and deformation capacity of RC columns and influences the performance of the bridge system as a whole. Torsion in bridges with outrigger bents occurs due to eccentricity of reaction force developed in the footing due to lateral movement of superstructure under seismic vibration (Fig. 1.a). In skewed bridges, the collision between bridge deck and abutment may cause in plane rotation of superstructures and consequently induces torsion in the bridge columns (Fig. 1.b). This implies the necessity to carry on a study on columns subjected to torsional loading under seismic activities. Till date most of the researches have been done on the torsional response of the columns (Hurtado, 2009) and very few studies on strengthening techniques of columns (S. T. Rutledge, 2012). Of those few studies, the research is limited to strengthening of columns under uniaxial eccentric loading (Hadi, 2005). There exists no study on strengthening of columns with FRP that are subjected to torsional loading. It is of major concern as under combined torsion and lateral loading concrete cracking predominantly changes from horizontal cracks associated with flexure to inclined cracks associated with torsion induced shear (Hurtado, 2009). The presence of torsion with shear and flexure increases the possibility of shear-dominated failure. This type of loading conditions occurs usually when bridge columns are subjected to seismic activities. Hence the present study focus on FRP strengthening of reinforced concrete (RC) columns (square and circular) under torsional loading in

order to fill the research gap. For this, a non-linear Finite Element (FE) models (square and circular columns) are generated in ABAQUS and numerical analysis are carried so as to predict the global and local behaviour of the columns wrapped with and without FRP. The overall torque-twist behaviour, tensile damage, strain and shear stress variations are observed. Later the analysis is carried on using SMMT-FRP model in MATLAB.

The overall torque-twist behaviour of the RC columns with and without FRP is observed and compared with FE model which has shown a good agreement. Then parametric study has been carried on by varying parameters like number of layers of FRP, thickness of FRP, orientation of FRP and by increasing axial load. The overall torque-twist behaviour is observed and plotted in all the cases. Torque-Axial load is plotted for the columns strengthened with and without FRP in order to understand the significance of FRP.

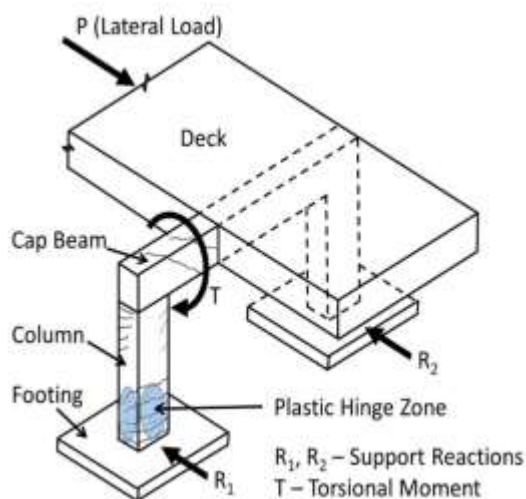


Fig (1.a) - Outrigger bent

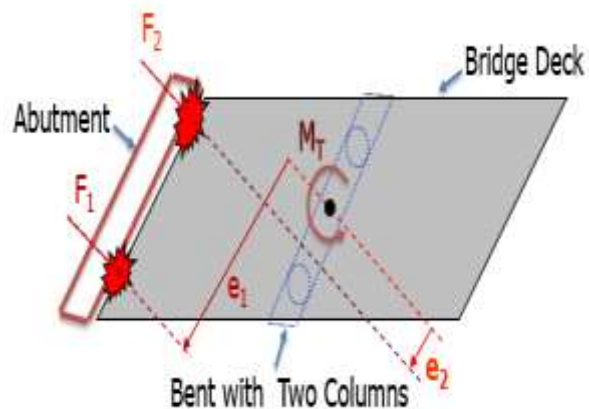


Fig (1.b) - Skewed Bridge

1.2 STRUCTURAL STRENGTHENING WITH FRP

COMPOSITES:

Composite materials are formed by the combination of two or more materials that retain their respective characteristics when combined together to achieve properties (physical, chemical, etc.) that are superior to those of individual constituents. The idea of combining two or more different materials resulting in a new material with improved properties exists from ages. The history of FRP composites can be traced back thousands of years to Mesopotamia (present day Iraq) which included the use of mud and straw in bricks and asphaltic bonded copper sheets and decorated inlays set with natural resins. The inclusion of metallic wires to reinforce non-metallic applications are many. For example, decorative organic plastic and paper pulp were used to make canes and umbrella handles in the late nineteenth century in Europe (Seymour and Deanin, 1986). Even though composite use dates back to the earliest civilizations, but the use of engineered composites has dramatically increased in the last century.

Fibre-reinforced composites are composed of at least two constituent materials differing in terms of thermomechanical properties, with combined properties engineered to be superior to constituent materials. The main components of composites are reinforcing agents and matrix. The fibres act as the reinforcement and provide most of the stiffness & strength. The matrix binds the reinforcement together thus effecting the load transfer from matrix to reinforcement. Fibre reinforced composites can be

further divided into those containing discontinuous or continuous fibres. Another commonly practiced classification is by the matrix used: polymer, metallic and ceramic. Here the study uses fibre reinforced composites with polymer matrix. The design of a structural component using composites involves both material and structural design. Unlike conventional materials like steel, the properties of the composite material can be designed considering the structural aspects. Composite properties like stiffness, thermal expansion, etc. can be varied continuously over a broad range of values under the control of the designer.

1.2.1 Advantages of Composites

Composites are able to meet diverse design requirements with significantly less weight as well as high strength-to-weight ratio as compared to conventional materials. Some advantages of composite materials over conventional one are:

1. Tensile strength of composites is four to six times greater than that of steel or aluminium.
2. It has improved torsional stiffness and impact properties
3. Composites have higher fatigue endurance limit (up to 60% of the ultimate tensile strength).
4. Composite materials are 30-45% lighter than aluminium structures designed to the same functional requirements
5. Lower embedded energy compared to other structural materials like steel, aluminium etc.

6. Composites are less noisy while in operation and provide lower vibration transmission than metals
7. Long life offers excellent fatigue, impact, environmental resistance and reduced maintenance
8. Composites exhibit excellent corrosion resistance

Commonly encountered engineering challenges such as increases in service loads, changes in use of the structure, design and/or construction errors, degradation problems, changes in design code regulations and seismic retrofits are some of the causes that led to the need for rehabilitation of existing structures. Complete replacement of an existing structure may not be a cost-effective solution and the structure is likely to be upgraded. In this context, strengthening with Fibre Reinforced Polymers (FRP) composite materials in the form of external reinforcement is of great interest to the civil engineering community. FRP composite materials are of great interest because of their superior properties such as high stiffness and strength as well as ease of installation when compared to other repair materials. Also, the non-corrosive and nonmagnetic nature of the materials along with its resistance to chemicals made FRP an excellent option for external reinforcement. Bridges account for a major sector of the construction industry. FRP has been found quite suitable for repair, seismic retrofitting and upgrading of concrete bridges as a way to extend the service life of existing structures. FRP is also being considered as an economic solution for new bridge structures.

1.3 NECESSITY FOR STRENGTHENING:

Now-a-days there has been a considerable increase in the occurrence of seismic activities. The addition of torsion in the skewed bridge columns or bridges with outrigger bents is very common because of its structural shape. During seismic activity, because of strong ground shaking considerable amount of lateral load acts on the column. This lateral load on combining with torsion changes the cracking pattern in concrete from horizontal cracks associated with flexure to inclined cracks associated with torsion induced shear (Hurtado, 2009). This increases the possibility of shear dominated failure mode, which is undesirable.

In addition, the presence of torsional loads limits the capacity of column to the spalling load (Prakash, 2009). Two processes are prerequisites for the spalling of concrete cover away from the concrete core. The first involves interface cracking between the concrete cover and the core; the second requires a driving mechanism to push the concrete cover away from the section. Although ultimate strength may or may not be affected by spalling, it definitely affects the serviceability requirements. A minimum thickness of concrete cover is recommended by various design codes. However, greater cover thickness will have adverse effects on the spalling if the member is subjected to shear or combined shear and torsion. If the principal tensile stress due to shearing stresses from torsional moment and shear force exceeds the tensile strength of the concrete, spalling of concrete cover occurs along the plane of weakness formed by the transverse reinforcement. Fig.1.c (Prakash, 2009) shows the variations in length of spalling zone with increase in torsional moment. A thick concrete cover increases

the possibility of spalling and leads to larger crack width and spacing (Rahal and Collins, 1995).

The above all mentioned research conclusions gives a clear view stating the necessity for strengthening of columns subjected to torsional loading. Here an attempt is made to strengthen the RC columns by wrapping with FRP under torsional loading.

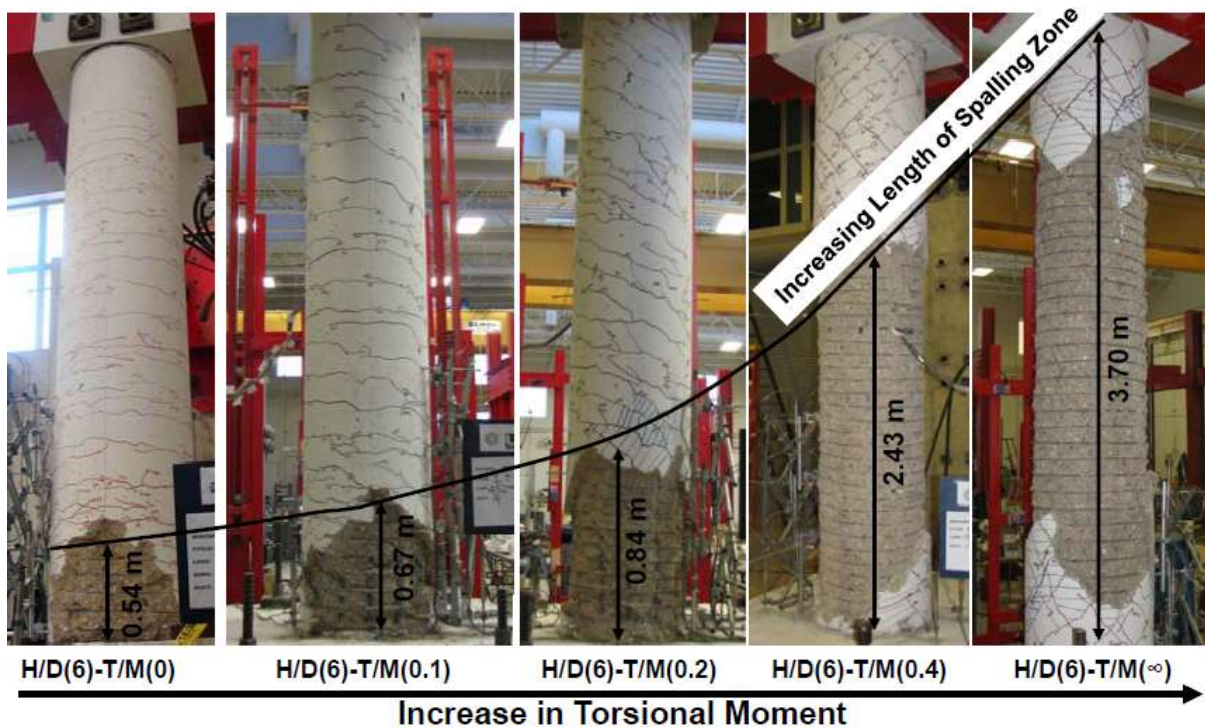


Fig (1.c) Variation of length of spalling zone with increase in Torsional Moment

1.4 RESEARCH MOTIVATION:

It is necessary to widen the knowledge in the field of strengthening the RC columns against seismic activities. The research done till now is mainly focussed on strengthening of columns by FRP under concentric or eccentric loading (Hadi, 2005) and a few studies on strengthening techniques of damaged RC circular columns with

FRP (Rutledge, 2012). But however no study has been carried on strengthening of RC columns by FRP under torsional loading in spite of its frequent occurrence in bridge columns under seismic activities. The current study focuses on filling this knowledge gap. For this, analytical and numerical analysis are carried on by using MATLAB and ABAQUS respectively. Initially, non-linear FE models are generated to predict the global as well as local behaviour of the RC square and circular columns with and without FRP. The non-linear FE models generated without FRP are validated with experimental results and the same is generated for the columns with FRP and the torque-twist behaviour, progress of the damage are observed. Later using Softened Membrane Model for Torsion with FRP (SMMT-FRP) analysis is carried for the RC circular columns strengthened with and without FRP. The overall torque-twist behaviour is observed for all the cases with and without FRP by varying parameters like number of layers of FRP, thickness of FRP, orientation of FRP and increasing axial load. Torque-Axial load variation is also plotted in order to understand the significance of FRP.

1.5 OBJECTIVES AND SCOPE:

Part-I:

The objective of this study is to understand the behaviour, damage distribution, failure progression of RC columns under torsion with and without strengthening using FRP composites.

The scope of the study are:

- To develop a FE model to predict the behaviour of RC columns (square and circular) under monotonic loading as a function of time and validating with experimental results.
- To develop FE model of RC columns (square and circular) strengthened with FRP to predict the behaviour under the same loading conditions.
- To observe the overall Torque-Twist behaviour for all cases.
- To predict the damage distribution and failure progression of RC columns under torsional loading.

Part-II:

The objective of the study is to understand the overall torque –twist behaviour of RC circular columns strengthened with FRP composites and to understand the significance of FRP by conducting varying parametric study.

The scope of the study are:

- To develop a matlab code based on Softened Membrane Model for Torsion with FRP (SMMT-FRP).
- To carry out the analysis of RC circular columns strengthened with and without FRP in order to predict the overall torque-twist behaviour.
- The same is validated with the Finite Element Analysis.
- To predict the overall torque-twist behaviour of RC circular columns strengthened with FRP by varying parameters like number of layers of FRP, thickness of FRP and alignment of FRP.

- To predict the Torque-Axial load behaviour by carrying the analysis on RC circular columns with and without FRP by varying the axial load.

The overall behaviour prediction of this work is limited to square and circular columns only. The parametric study is limited to only circular columns only. The parametric studies conducted for circular columns can also be done for columns of any shape is scope of future study.

CHAPTER-2

LITERATURE

REVIEW

CHAPTER-2

LITERATURE REVIEW

2.1 BEHAVIOR OF RC COLUMNS UNDER TORSION:

Seismic torsion in bridges in the past earthquakes has been analytically investigated (Hurtado 2009, Mondal and Prakash 2015c) and experimentally measured (Hurtado 2009, Prakash 2009) by different researchers. These studies emphasizes on the occurrence of torsional rotation in bridge structures during strong ground shaking and that torsion should be taken into consideration when designing the supporting bridge columns.

Hurtado (2009), carried both analytical and experimental study on RC columns. His key findings includes that: Under combined torsion and lateral loading concrete cracking changed from predominantly horizontal cracks associated with flexure to inclined cracks associated with torsion induced shear. It also increased the strain demands on the hoop reinforcement leading to earlier yielding of hoops. Analytical models are developed to understand the effect of twist on column response and to investigate the degree of twist anticipated for simplified bridge structures.

Prakash (2009) carried an analytical and experimental study for better understanding of seismic behaviour of circular RC bridge columns under combined loading. The experimental investigation tested 14 circular RC columns under various

T/M ratios and bending moment-to-shear ratios. The key findings of the study are: (i) Columns subjected to pure torsion failed by severe diagonal cracking, leading to the formation of a torsional plastic-hinge near the mid-height of the column. (ii) The location and length of the plastic-hinge change with specific combinations of bending and torsion, i.e., with changes in the T/M ratio. (iii) A combination of bending and torsional moments reduces the torsional moment required to cause yielding of the transverse reinforcement and the peak torsional strength. (iv) Under combined torsion and bending, torsional stiffness degrades more rapidly than flexural stiffness with the increments of displacement or twist in columns. (v) Increase in spiral reinforcement ratio improves torsional strength and twist ductility with increase in deformational capacity after yielding. (vi) An increase in the spiral ratio also provides more confinement thereby reducing the damage index for flexure and torsional hysteresis under combined loading.

Mondal and Prakash 2015c, carried an analytical study on RC columns under torsion with and without axial compression by generating a non-linear FE models in order to predict the behaviour of column under those loading conditions. The key findings of this study are:

An increase in transverse steel ratio was found to increase the torsional capacity and limit the damage of columns under torsion. It was further observed that at a low level of axial compression, the torsional capacity of columns is enhanced. The shape of the cross section is found to play a major role in the distribution of torsional damage in

the columns. Square columns exhibited a more localized damage due to presence of warping, whereas circular columns exhibited damage distributed along their length.

2.2 BEHAVIOR OF RC BEAMS UNDER TORSION:

Mitchell and Collins (1974) observed the detailing consequences of the longitudinal and transverse reinforcement in beams. The study states that the primary function of the longitudinal steel and hoops is to hold the beam tightly along its axis and in lateral directions respectively. By laboratory test they also showed that, in general, as the hoop spacing and the longitudinal bar spacing were increased, the crack spacing and width are also increased.

Hsu (1968a) investigated the behaviour of reinforced concrete rectangular beams under pure torsion by conducting tests on nine series of beams. The eight major variables that were considered in the study were (a) amount of reinforcement (b) solid beam versus hollow beams (c) ratio of volume of longitudinal bars to volume of hoops (d) concrete strength (e) scale effects (f) depth to width ratio of cross section (g) spacing of longitudinal bars and (h) spacing of hoops. Some of the significant key findings of his study were: Before cracking, the behaviour of reinforced concrete beam was identical to its corresponding plain concrete beam with no effect from reinforcement. But however the amount of reinforcement did affect the cracking torque generally increasing with increasing reinforcement.

2.3 FRP STRENGTHENED BEAMS:

The experimental and numerical study was carried (Ameli et al. 2007) to predict the behaviour of FRP strengthened reinforced concrete beams under torsion. The key findings of the study were: (i) The pattern of concrete cracks in the strengthened beams have a wider spread along the length compared to individual cracks. (ii) It is also observed that the crushing signs at ultimate for strengthened beams is more distributed. (iii) Experimental results show that FRP wraps can increase the ultimate torque of fully wrapped beams considerably in addition to enhancing the ductility. (iv) Two batch of beam tests were carried on with Carbon FRP (CFRP) and Glass FRP (GFRP) which shows that CFRP materials increased the strength more than GFRP but failed immediately after reaching the peak, whereas GFRP gives an appreciable post peak response. This proves that GFRP is preferable for strengthening of structural elements where the ductility demand is high i.e., to strengthen the elements under seismic activities.

The study conducted by Belarbi and Panchacharam (2002) investigated the torsional behaviour of the reinforced concrete beams strengthened with externally wrapped GFRP sheets by including the variables such as fibre orientation (parallel and perpendicular to the longitudinal axis of the beam), FRP continuous wrap or strips, etc. The key findings of the study are:

Torsional reinforced concrete beams strengthened with GFRP sheets exhibited significant increase in their cracking and ultimate strength as well as ultimate twist deformations. Strengthening schemes with complete wraps in 90-degree fibre

orientation with respect to beam axis provided an effective confinement and therefore resulted in a significant increase (about 150%) in the ultimate torsional strength. Substantial increase in cracking strength was observed when RC beams were strengthened with FRP sheets oriented in the longitudinal direction of the beam. There was an increase in both the ultimate strength, post-cracking torsional twist and ductility of the beam when FRP sheets are wrapped all-around in the form of strips oriented in the longitudinal direction of the beam.

2.4 BEHAVIOR OF FRP STRENGTHENED RC

COLUMNS:

A very few studies have been done on strengthening techniques of RC columns with FRP (Rutledge et al. 2012; Hadi, 2005).

Rutledge et al. (2012) carried a study on repair of RC columns with FRP by relocating plastic hinge. The study made an attempt to restore sufficient strength to damaged RC columns, which contain buckled longitudinal reinforcement. The attempt was made successful by relocating the plastic hinge by making use of unidirectional CFRP sheets oriented in the vertical and hoop directions. After the relocation of the plastic hinge, the confinement of a repaired region showed an increase in the performance in terms of force and displacement capacity.

Hadi (2005) carried a study on behaviour of FRP wrapped normal strength concrete columns under eccentric loading. Columns that are in the border of buildings, especially corner columns and columns near opening are usually subject to a

combination of axial load and bending moment, thus creating an equivalent eccentric load. In this study, six eccentrically loaded concrete columns tested by wrapping them with FRP. The key findings of the study are: The addition of external confinement to plain specimens, in various layered formats, significantly improved behaviour in ductility. It is suggested to use minimum of three layers of FRP for normal strength concrete in order to achieve significant structural gains in structures.

Besides all these studies on torsional behaviour, damage of columns under seismic activities, strengthening of columns by FRP still there exists a gap in knowledge like how to strengthen the RC columns under torsional loading, which is quite often a common issue in bridge structures. The current study focuses to build up this knowledge gap by my making use of FRP.

CHAPTER-3

FINITE ELEMENT

ANALYSIS

CHAPTER-3

FINITE ELEMENT ANALYSIS

3.1 INTRODUCTION

Finite element analysis of RC structures has gained a considerable attention in the recent years. But however no finite element analysis has been carried on RC columns subjected to torsional loading in spite of its occurrence in bridge columns under seismic activities. This study aims at conducting a finite element analysis of RC circular and square columns strengthened with and without FRP under torsional loading by generating a nonlinear FE models. The local and global behaviour of the FE models without FRP is validated with test data. The same models are regenerated and analysed by strengthening with FRP. The overall torque twist behaviour is well captured. In addition, FE models showed a good agreement on damage mechanism and progression of failure when calibrated with test data. Thus the developed models are assumed to give an appropriate behaviour for the RC columns that are strengthened with FRP which don't have any test data to validate.

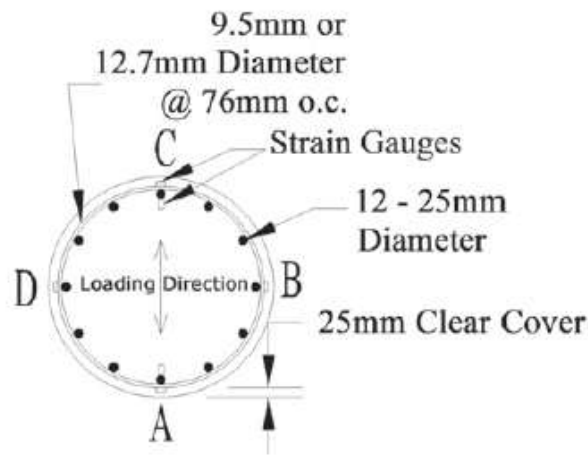


Fig.3.1 (a) H/D (6)-T/M (∞)-0.73%

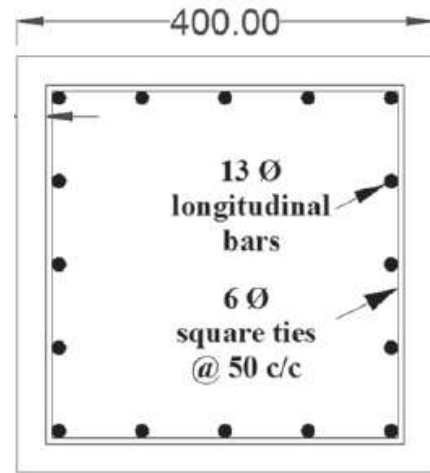


Fig.3.1 (b) TP-91

Fig.3.1 Cross Section of the specimens

Table-1 Specimen Details:

<i>Specimen Id</i>	<i>H/D(6)-T/M(∞)-0.73%</i>	<i>TP-91</i>
<i>Section Shape</i>	Circular	Square
<i>Diameter/Width (mm)</i>	610	400
<i>Clear Cover (mm)</i>	25	27.5
<i>Total Column Height (m)</i>	4.55	1.75
<i>Effective Column Height (m)</i>	3.65	1.35
<i>Cylinder Strength of Concrete (MPa)</i>	37.90	28.3
<i>Longitudinal Steel Yield Strength (MPa)</i>	462	354
<i>Transverse Steel Yield Strength (MPa)</i>	457	328
<i>Transverse Steel Ratio (percentage)</i>	0.73	0.79
<i>Longitudinal Steel Ratio (percentage)</i>	2.1	1.27
<i>Axial Force (kN)</i>	600.51	0

3.2 ELEMENTS:

Concrete was modelled with the *C3D8R* element, which is a 3D eight noded linear brick element with three translational degrees of freedom at each node. Rotational degrees of freedom are expressed in terms of the translational degrees of freedom. *T3D2* element was used to model the rebar's. It is a two noded 3D truss element with three translational degrees of freedom at each node. FRP is modelled using *S4R* element which is 4-noded doubly curved thin shell element.

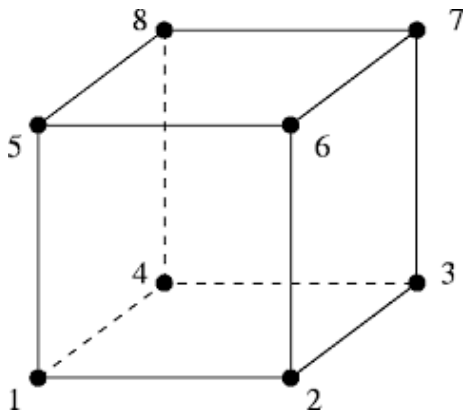


Fig 3.2 (a) C3D8R element

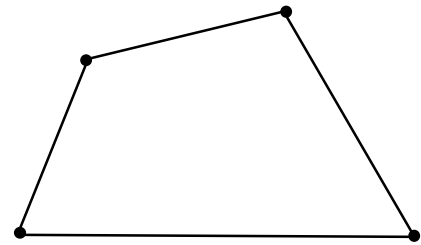


Fig 3.2(b) S4R element

3.3 MATERIAL MODELS:

3.3.1 Concrete – Damage Plasticity Model:

Concrete is a quasi-brittle material and has different behaviour in compression and tension. The smeared crack approach and damaged plasticity approach are generally used for nonlinear analysis of concrete. In this study, the damaged plasticity approach has been adopted because it offers a broad potential for matching the

simulation results to experimental values (Mondal and Prakash, 2015c). This model uses concepts of isotropic damaged elasticity in combination with isotropic tensile and compressive plasticity to represent the inelastic behaviour of concrete. This model is highly suitable for the analysis of RC structures subjected to monotonic or cyclic dynamic loading under low confining pressure. The details of this model can be found in ABAQUS analysis user's manual, 6.11.

The model is a continuum, plasticity-based, damage model for concrete. It assumes that there are mainly two failure mechanisms called as tensile cracking and compressive crushing of the concrete material. The evolution of the yield (or failure) surface is controlled by two hardening variables and linked to failure mechanisms under tension and compression loading. The model assumes that the uniaxial tensile and compressive response of concrete is characterized by damaged plasticity.

The values of Young's modulus and Poisson's ratio were provided as elastic properties. For the nonlinear part, compressive stress data are provided as a tabular function of inelastic (or crushing) strain to define the hardening behaviour of concrete under compression. The tension-stiffening option was used to define the strain-softening behaviour of concrete after cracking. Tension stiffening can be specified by means of post cracking yield stress and cracking strain values. It helps in approximately modelling of the bond behaviour between steel and concrete. The absence of tension stiffening could lead to local cracking failure, which could introduce temporary instability in overall response of the model. Hence, it is important to define tension

stiffening from the perspective of numerical stability. The variation of the damage variables with stress states were also specified under tension and compression.

The compressive stress–strain model proposed by Vecchio and Collins (1986) was used to model concrete in this study. The behaviour is linearly elastic up to about 30% of the maximum compressive strength. Above this point, the stress increases gradually up to the maximum compressive strength. Once it reaches the maximum compressive strength, the curve descends into a softening region, and eventually crushing failure occurs when ultimate strain is reached.

The stress–strain curve for concrete under tension is approximately linearly elastic up to the maximum tensile strength. After this point, the concrete cracks and the strength decreases gradually to zero. Several tension-stiffening models are available to model the strain softening observed in cracked concrete.

The default values of the failure ratios were taken from the literature (Mondal and Prakash, 2015c). The dilation angle was assumed to be 36° . The ratio of the ultimate biaxial compressive stress to the ultimate uniaxial compressive stress was taken as 1.16. The absolute value of the ratio of uniaxial tensile stress at failure to the uniaxial compressive stress at failure was assumed to be 0.1, although the default value is 0.09. The value of the viscosity parameter was assumed to be zero.

The dimensions, properties of the circular column modelled are taken from Prakash (2009) and for square columns the same is taken from Tirasit and Kawasima (2007a, 2007b).

3.3.2 Steel

Stress – strain behaviour of steel was obtained from coupon tests conducted by Prakash (2009) for circular columns and the same for square columns by Tirasit and Kawasima (2007a, 2007b). Mass density was taken as 7800 kg/m³. Modulus of elasticity and Poisson's ratio were assumed to be 200000 MPa and 0.3 respectively.

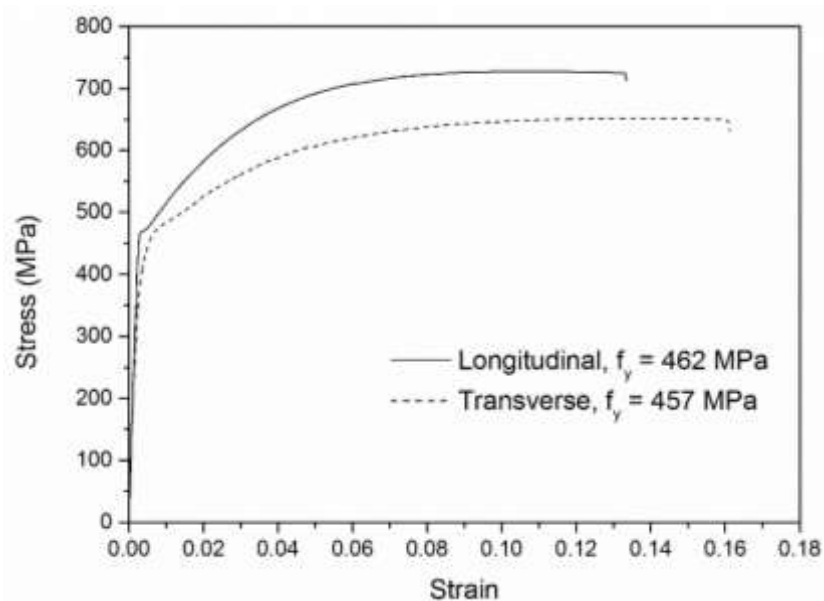


Fig.3.3.2 Coupon test results for steel used in the circular columns

3.3.3 FRP:

In this study, Glass Fibre reinforced polymer (GFRP) is used. CFRP materials increase the strength more than GFRP but fails immediately after reaching the peak, whereas GFRP gives an appreciable post peak response (Ameli et al. 2007). For strengthening of columns subjected to torsional loading, ductility is one of the major factor to be considered. Hence GFRP is chosen over CFRP. The properties of FRP are taken from Suman (2015). The properties are as mentioned in Table-2.

Table-2 Properties of unidirectional FRP sheets used in the Finite Element study

<i>Type of FRP</i>	<i>Thickness (mm)</i>	<i>Modulus of elasticity (MPa)</i>	<i>Tensile Strength (MPa)</i>
GFRP	1	28000	696

3.4 PROCEDURE – DYNAMIC EXPLICIT:

Any quasi-static problem can be solved as a dynamic one with sufficiently slow load increments to produce negligible inertial force. An available explicit integration scheme is used in this study owing to its advantages for highly nonlinear problems (Zimmermann 2001).

Robustness in convergence behaviour, numerical stability, low computation cost, and suitability for calculation in the post failure range are the advantages of the explicit integration method. If dynamic analysis is adopted for a static or quasi-static procedure, the ratio of kinetic energy to internal energy (ALLKE: ALLIE) must be less than 0.1, as recommended by Zimmermann (2001). This condition was satisfied for all specimens considered in this study.

3.5 STEEL – CONCRETE INTERFACE:

The reinforcing steels are embedded as bar element. The steel rebar's which are modelled as separate truss elements can also be connected to the surrounding concrete

elements through interface elements. This approach is capable of representing the bond stress–slip relations between reinforcement and concrete. To improve the predictions, bond slip behaviour was modelled at the interface between longitudinal steel and concrete using a surfaced based contact interaction model. This Penalty interaction algorithm uses Coulomb friction model (ABAQUS Analysis User’s Manual 6.11) for surface to surface interactions. The value of coefficient of friction was assumed to be 0.6 as suggested by Rabbat and Russell (1985). Shear stress limit was taken from Floros and Ingason (2013). Elastic slip stiffness was obtained from an equation proposed by Delso et al. (2011). Number of parametric studies was carried out to study the influence of bond on torsional behaviour. Incorporation of bond slip model did not produce appreciable improvement in the results when compared to perfect bond model. Hurtado (2009) observed that there was negligible slip during the testing of RC columns under torsion, unlike in flexure, where the slip is considerable. Hence, a perfect bond was considered for modelling the steel–concrete interface in all the models to reduce the computational time.

3.6 LOAD AND BOUNDARY CONDITIONS:

Load and boundary conditions have significant influence on FE solutions. In this study, all degrees of freedom are restrained at the bottom of the column. The top portion is provided to deform in any mode under rigid body condition. The relative positions of the regions that are part of the rigid body remain constant throughout the analysis. A reference point was created at the centre of the surface and was assigned as the rigid-body reference point. Motion or constraints applied to the reference point are then

applied to the entire rigid part. The angle of rotation was imposed monotonically at the reference point as a function of time in a tabular form. For circular column FE analysis a constant magnitude of axial compressive load was also applied at the same reference point to simulate the experimental study's test conditions. The constant axial load applied on the circular columns is very less compared to the dimension of the column. Hence it has very less significance and can be considered as a case under pure torsion.

3.7 MESHING

The accuracy of FE results greatly depend on the size of the mesh, the kind of element used, and the order of approximation. The type of elements used for concrete, steel and FRP are respectively mentioned in 3.1 Elements. Reduced integration was used to eliminate excess stiffness due to shear locking. Hourglass control was adopted to eliminate the spurious modes. The linear elements are used in this study which require finer mesh, leading to an increase in demand for computer capacity. However, this rise in capacity requirement is offset by the explicit integration scheme, which is compatible to larger mesh sizes. To result in finer mesh sizes, the number of elements was increased, keeping the aspect ratio constant. This process was repeated successively until convergence of results was achieved.

CHAPTER-4

SOFTENED MEMBRANE

MODEL FOR TORSION-FRP

CHAPTER-4

SOFTENED MEMBRANE MODEL FOR TORSION WITH FRP (SMMT-FRP)

4.1 INTRODUCTION:

In typical design practices, the torsional moment is generally ignored. However, previous investigations revealed that the presence of torsional loading significantly affects the strength and stiffness of the columns under axial and lateral deformations. Furthermore, torsional loading might result in brittle shear failure and trigger catastrophic failure of the structure. All these conditions necessitates a deeper understanding of the torsional response of RC bridge columns. Till date, the studies have been carried on torsional response of RC bridge columns subjected to torsion but no study has been conducted on torsional response of FRP strengthened RC bridge columns. Here my study focuses on understanding the torsional behaviour of FRP strengthened RC bridge columns subjected to torsion. In addition, parametric studies were carried out by varying the layers and orientation of FRP, increasing the axial load for the columns with and without FRP in order to understand the significance of FRP.

4.2 SOFTENED MEMBRANE MODEL FOR TORSION:

Softened Membrane Model (SMM) was first developed by Hsu and Zhu (2002) to predict the behaviour of RC membrane elements under shear, including the effect of bidirectional stress states, which was actually ignored in the Softened Truss Model (STM). The traditional truss concept is the underlying philosophy for the SMM, in which compressive stresses are taken by the concrete struts and tensile stresses are taken by the longitudinal and transverse reinforcing bars after cracking. Later Jeng and Hsu (2009) extended SMM to RC membrane elements subjected to torsion and proposed a theory by name Softened Membrane Model for Torsion (SMMT). In this model Jeng and Hsu (2009) have taken into account the strain gradient of concrete struts in the shear flow zone by modifying the constitutive relationships of concrete. They observed that the strain gradient that arises from bending concrete struts under torsional loading leads to higher tensile strength and stiffness than those under shear state in a membrane element. The behaviour of circular and noncircular sections under torsion is very different because of changes in shear flow characteristics and warping. In the case of square/rectangular columns, the strain-gradient effect is significant due to warping of the cross section. However, the strain-gradient effect in circular sections is not very significant as that in case of rectangular sections. Therefore, the tension–stiffening relationship proposed by Jeng and Hsu (2009) for noncircular sections cannot be used directly for circular sections. In order to incorporate this correction, Anand et al. (2015) developed a new tension stiffening model by modifying the descending/post peak part of the tensile constitutive law for concrete. Later the same author developed

an improved softened membrane model (SMMT-FRP) considering the influence of FRP composites on the compressive behaviour of cracked concrete. A new tension stiffening relationship of concrete is also recommended which also included bidirectional stress states in its formulations. But the SMMT-FRP model proposed by Anand.et.al (2015) is limited to rectangular sections. This study has put together all the modifications required in the existing SMMT-FRP model by making use of theories developed by Jeng and Hsu (2009) and Anand.et al. (2015) to make it applicable for circular sections. The analytical study had been carried on to predict the behaviour of RC circular bridge columns strengthened with and without FRP under torsional loading using MATLAB.

4.3 SOFTENED MEMBRANE MODEL FOR TORSION WITH FRP (SMMT-FRP)

SMMT-FRP model is an extension of basic SMMT theory proposed by Jeng and Hsu (2009), where the effect of FRP is included by considering the constitutive relationship of concrete in compression due to the effect of FRP strengthening. It is developed by Anand.et al. (2015). This model is based on the popular truss concept for cracked reinforced concrete, which was developed based on three Navier's principles of mechanics that are discussed in the following sections.

4.3.1 Navier's Principles of Mechanics:

4.3.1.1 Stress Equilibrium Equations:

When an RC prismatic member is subjected to an external torque T as shown in Fig.4.3.1 (a), the external torque is resisted by an internal torque formed by the circulatory shear flow q . This shear flow q occupies a shear flow zone, with an effective thickness t_d . The element A in the shear flow zone is subjected to a shear stress.

Concrete is fully effective in resisting the applied torque before cracking. Once the applied torque reaches the cracking torque, steel and FRP become effective in resisting the applied torque. Membrane element subjected to in plane stresses and respective stress components of concrete, steel and FRP is shown in Fig.4.3.1 (b). Stress equilibrium equations for the membrane element are represented in Eqns. (1) (2) & (3).

$$\sigma_1 = \sigma_{1c} \cos^2 \alpha + \sigma_{2c} \sin^2 \alpha - 2\tau_{12c} \sin \alpha \cos \alpha + \rho_l f_l + \rho_{fl} f_{fl} \quad (1)$$

$$\sigma_t = \sigma_{1c} \sin^2 \alpha + \sigma_{2c} \cos^2 \alpha + 2\tau_{12c} \sin \alpha \cos \alpha + \rho_t f_t + \rho_{ft} f_{ft} \quad (2)$$

$$\tau_{lt} = (\sigma_{1c} - \sigma_{2c}) \sin \alpha \cos \alpha + \tau_{12c} (\cos^2 \alpha - \sin^2 \alpha) \quad (3)$$

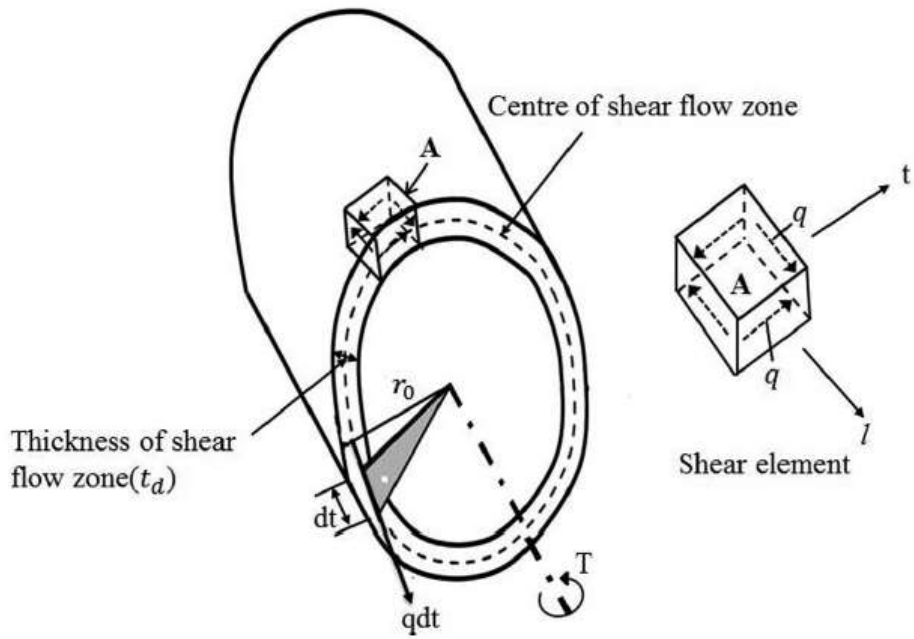


Fig.4.3.1 (a) R.C section and shear element subjected to torque and in plane shear flow

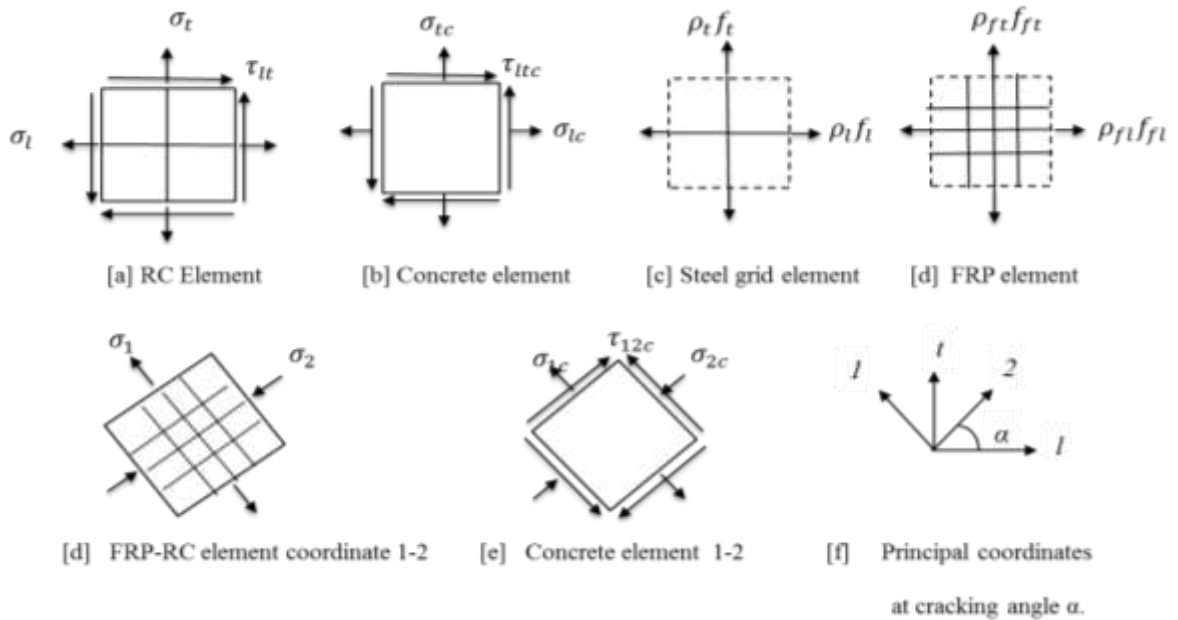


Fig.4.3.1 (b) FRP-RC membrane element subjected to in-plane stresses under torsion

4.3.1.2 Strain Compatibility Equations:

In-plane strain compatibility should be satisfied for all the membrane elements. The compatibility conditions that relate the strains in steel and concrete are given by the following Eqns. (4) -(6)

$$\varepsilon_l = \varepsilon_1 \cos^2 \alpha + \varepsilon_2 \sin^2 \alpha - \gamma_{12} \sin \alpha \cos \alpha \quad (4)$$

$$\varepsilon_t = \varepsilon_1 \sin^2 \alpha + \varepsilon_2 \cos^2 \alpha + \gamma_{12} \sin \alpha \cos \alpha \quad (5)$$

$$\gamma_{lt} = (\varepsilon_1 - \varepsilon_2) 2 \sin \alpha \cos \alpha + \gamma_{12} (\cos^2 \alpha - \sin^2 \alpha) \quad (6)$$

4.3.2 Constitutive Laws of Materials:

4.3.2.1 Constitutive relationship of concrete in compression:

4.3.2.1.1 Softening effect of concrete:

The presence of tensile cracks in the principal compression plane softens the stress–strain behaviour of concrete struts. The softening coefficient (ζ) is one of the most important parameter affecting the compressive stress–strain relationship of cracked reinforced concrete. In this model also a compressive stress strain relationship of softened concrete is employed, as in the case of SMM. Vecchio and Collins (1986) found that softening is a function of principal tensile strain. Zhang (1995) found that the softening coefficient (ζ) is also a function of the compressive strength of concrete

(f_c') . Wang (2006) investigated the influence of the deviation angle (β) on softening of concrete and proposed a modified softening coefficient. The softening coefficient, which includes all three factors mentioned above was used in SMMT by Jeng and Hsu (2009). The softening coefficient which is a function of three variables: the uniaxial tensile strain ($\bar{\varepsilon}_1$) in the perpendicular direction, the concrete compressive strength (f_c') and the deviation angle (β) is as follows:

$$\zeta = f_1(\bar{\varepsilon}_1)f_2(f_c')f_3(\beta)$$

Where

$$f_1(\bar{\varepsilon}_1) = \frac{1}{\sqrt{1 + 400\bar{\varepsilon}_1}}$$

$$f_2(f_c') = \frac{5.8}{\sqrt{f_c'}}$$

$$\beta = \frac{1}{2} \tan^{-1} \left[\frac{\gamma_{12}}{(\varepsilon_1 - \varepsilon_2)} \right] \quad (7a)$$

$$f_3(\beta) = 1 - \frac{|\beta|}{24^0}$$

Hence

$$\zeta = \left(\frac{5.8}{\sqrt{f_c'}} \right) \left(\frac{1}{\sqrt{1 + 400\bar{\varepsilon}_1}} \right) \left(1 - \frac{|\beta|}{24^0} \right) \quad (7b)$$

4.3.2.1.2 Strain gradient effect:

In a shear member, the principal compressive stress and the principal tensile stress remain constant across the thickness of membrane elements because of the absence of any out-of-plane deformation. However, in a torsional member, the angle of twist (θ), produces warping in the wall of the member, which in turn causes bending in the diagonal concrete struts. However, the presence of warping in circular members would be lesser when compared to that in rectangular sections, nevertheless it cannot be ignored. Circular RC members after cracking would be subjected to some warping stresses due to differences in the ratios of longitudinal and transverse reinforcements and by virtue of concrete being an inelastic material. SMMT proposed by Jeng and Hsu (2009) is for rectangular sections (noncircular sections). Later Anand et al (2015) proposed a modified SMMT model for circular sections in order to incorporate this correction. The warped shape of a membrane element is idealized as a hyperboloid surface (Fig. 4.3.2.1 (a), OGDH). The diagonals OD and GH in Fig.4.3.2.1 (a) are aligned in principal tension and compression directions, respectively. Rectangles abcd and efgh in Fig.4.3.2.1 (b) (a and b) represent the unit width of cross sections of the concrete strut perpendicular to Directions 2 and 1. A strain gradient, which influences the behaviour of the membrane element, can be seen in the principal directions.

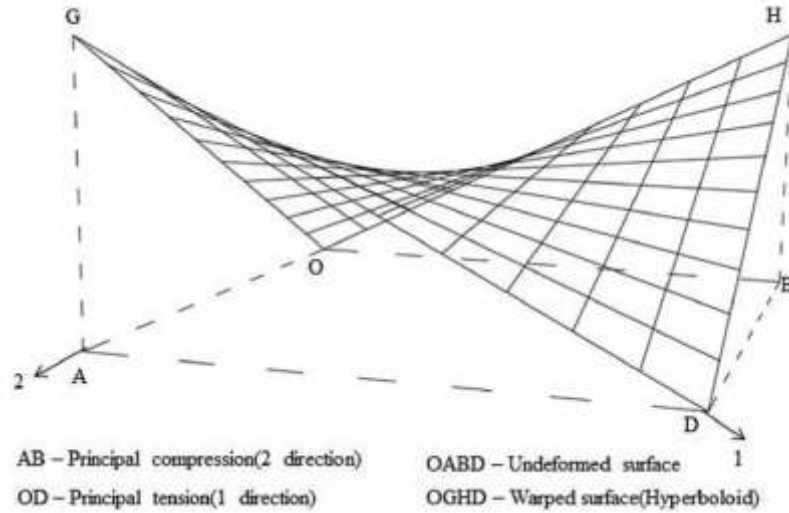


Fig.4.3.2.1 (a) Warped hyperboloid surface along 1 and 2 directions

4.3.2.1.3 Confinement effect of FRP:

Confinement effect due to the presence of FRP will counteract the softening effect. To incorporate this an additional coefficient f_4 (FRP) developed by Anand et al (2015) is used. This confinement coefficient is a function of smeared principal tensile strain, modulus of elasticity and thickness of FRP sheets.

$$f_4(FRP) = \left[1 + \left(\frac{E_{FRP}}{6890} \right) \left(\frac{t_{FRP}}{0.27} \right)^{\frac{2}{3}} (\bar{\epsilon}_1) \right] (1.12 - 16\bar{\epsilon}_1) \quad (8)$$

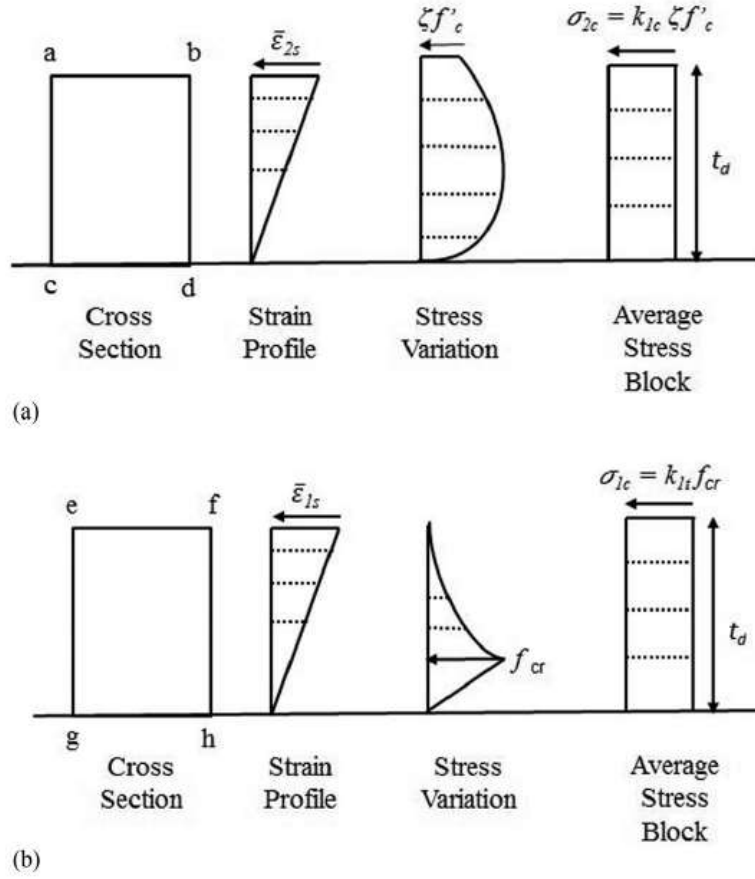


Fig.4.3.2.1 (b) Strain gradient effect along the principal directions.

(a) Direction-2 (principal compression) (b) Direction-1 (principal tension)

$$\sigma_{2c} = k_{2c} \zeta f_4(FRP) f'_c \quad (9)$$

$$k_{2c} = \left[\frac{\bar{\epsilon}_{2s}}{\zeta \epsilon_0} - \frac{(\bar{\epsilon}_{2s})^2}{3(\zeta \epsilon_0)^2} \right] \quad \left(\frac{\bar{\epsilon}_{2s}}{\zeta \epsilon_0} \leq 1 \right) \quad (10a)$$

$$k_{2c} = 1 - \frac{\zeta \epsilon_0}{3\bar{\epsilon}_{2s}} - \frac{1}{3\bar{\epsilon}_{2s}} \left[\frac{(\bar{\epsilon}_{2s} - \zeta \epsilon_0)^3}{(4\epsilon_0 - \zeta \epsilon_0)^2} \right] \quad \left(\frac{\bar{\epsilon}_{2s}}{\zeta \epsilon_0} > 1 \right) \quad (10b)$$

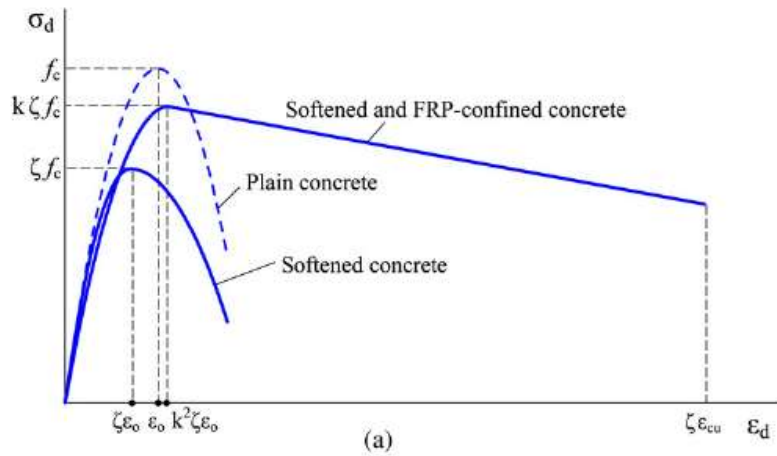


Fig.4.3.2 (a) Compressive stress strain curve of concrete

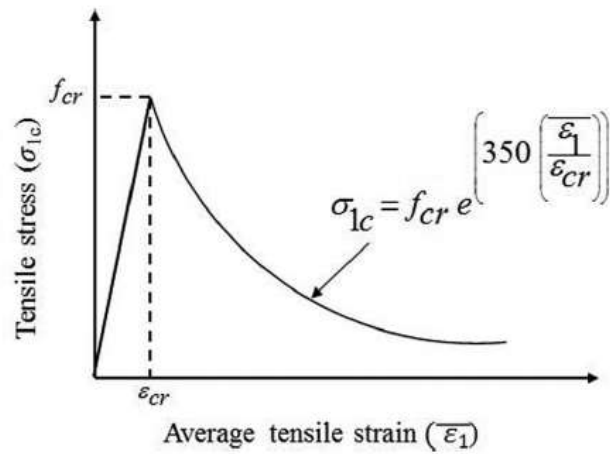


Fig.4.3.2 (b) Tensile stress-strain curve of concrete

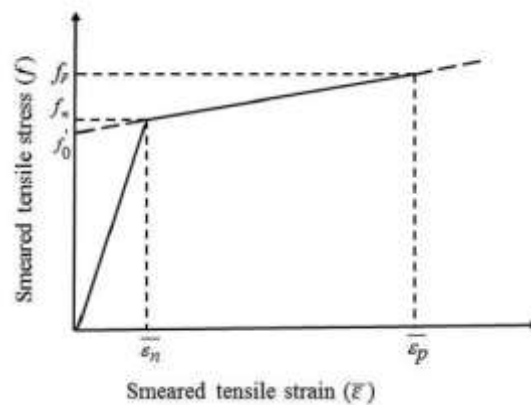


Fig.4.3.2 (c) Stress-strain behaviour of steel

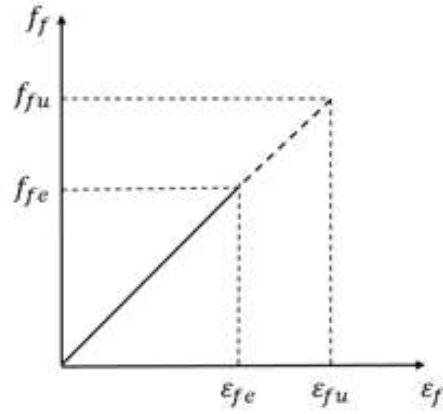


Fig.4.3.2 (d) Stress-strain behaviour of FRP

4.3.2.2 Constitutive relationship of concrete in tension:

Belarbi and Hsu (1994) proposed a tension stiffening relation for concrete, which was later modified by Jeng and Hsu (2009) to take the effect of strain gradient into account. Later Anand.et.al (2015) modified the tension stiffening relation by combining the models of Jeng and Hsu (2009) and Mondal and Prakash (2015). This modified tension stiffening relation is used in this study.

$$f_{cr} = 0.652\sqrt{f_c'} \quad (11)$$

$$E_c = 5620\sqrt{f_c'} \quad (12)$$

$$k_{1c} = \frac{1}{\bar{\epsilon}_{1s} f_{cr}} \int_0^{\bar{\epsilon}_{1s}} \sigma_{1c}(\bar{\epsilon}_1) d\bar{\epsilon}_1 \quad (13)$$

$$\sigma_{1c} = E_c \bar{\epsilon}_1 \quad \left(\frac{\bar{\epsilon}_{1s}}{\epsilon_{cr}} \leq 1 \right) \quad (14a)$$

$$\sigma_{1c} = f_{cr} e^{(350(\epsilon_{cr} - \bar{\epsilon}_1))} \quad \left(\frac{\bar{\epsilon}_{1s}}{\epsilon_{cr}} > 1 \right) \quad (14b)$$

4.3.2.3 Constitutive relationship of mild steel bars embedded in concrete:

The smeared stress strain curve of the steel embedded in concrete is shown in Fig.5.1.3 (c). The same material model was used for both transverse and longitudinal steel.

4.3.2.3.1 Longitudinal steel reinforcement:

$$f_l = E_{sl}\bar{\epsilon}_l \quad \bar{\epsilon}_l < \bar{\epsilon}_{ln} \quad (15a)$$

$$f_l = \left[(0.91 - 2B) + (0.02 + 0.25B) \frac{\bar{\epsilon}_l}{\epsilon_{ly}} \right] \quad \bar{\epsilon}_l \geq \bar{\epsilon}_{ln} \quad (15b)$$

$$B = \left[\frac{(f_{cr}/f_{ly})^{1.5}}{\rho_l} \right] \quad (15c)$$

$$\bar{\epsilon}_{ln} = \epsilon_{ly}(0.93 - 2B) \quad (15d)$$

4.3.2.3.2 Transverse steel reinforcement:

$$f_t = E_{st}\bar{\epsilon}_t \quad \bar{\epsilon}_t < \bar{\epsilon}_{tn} \quad (16a)$$

$$f_t = \left[(0.91 - 2B) + (0.02 + 0.25B) \frac{\bar{\epsilon}_t}{\epsilon_{ty}} \right] \quad \bar{\epsilon}_t \geq \bar{\epsilon}_{tn} \quad (16b)$$

$$B = \left[\frac{(f_{cr}/f_{ty})^{1.5}}{\rho_t} \right] \quad (16c)$$

$$\bar{\epsilon}_{tn} = \epsilon_{ty}(0.93 - 2B) \quad (16d)$$

4.3.2.4 Constitutive relationship of FRP:

The stress-strain behaviour of FRP under uniaxial tension is shown in the Fig.5.1.3 (d). The behaviour is assumed to be linearly elastic up to failure. The constitutive relationship of FRP under tension is as follows.

$$f_{fe} = E_{frp}\epsilon_{fe} \quad (17)$$

4.3.2.5 Constitutive relationship of concrete in shear:

Experimental investigation on constitutive relationship for concrete in pure 2D shear is difficult and for 3D shear in torsion is furthermore difficult. Therefore, a rational shear modulus is incorporated in the SMMT to relate the concrete shear stress to the shear strain as follows:

$$\tau_{12c} = \frac{\sigma_{1c} - \sigma_{2c}}{2(\epsilon_1 - \epsilon_2)}\gamma_{12} \quad (18)$$

4.3.3 Additional equations for torsion:

4.3.3.1 Thickness of shear flow zone(t_d):

In a torsional member, the angle of twist ϑ also produces warping in the wall of the member, which, in turn, causes bending in the concrete struts. In other words, the concrete struts are not only subjected to compression due to circulatory shear but also subjected to bending due to warping of the wall. Eqn. (18b) represents the relation between the angle of twist, ϑ and bending curvature of concrete struts (ψ).

The curvature ψ produces a non-uniform strain distribution in the concrete struts. Fig.4.3.3 (a) shows a unit width of a concrete strut in a hollow section with a wall thickness h . The tension area in the inner portion of the cross-section is neglected. The area in the outer portion that is in compression is considered to be effective to resist the shear flow. The depth of the compression zone from the neutral axis (N.A.) to the extreme compression fibre is defined as the thickness of the shear flow zone (t_d). Within this thickness (t_d), the strain distribution is assumed to be linear, as shown in Figure Fig.4.3.3 (b) Unlike RA-STM simplified expression for t_d is proposed in SMMT model in order to avoid iterative calculations. Thickness of shear flow zone (t_d) is related to curvature (ψ) and the maximum strain at the surface ε_{2s} as shown in Eqn. (18a)

$$t_d = \frac{\bar{\varepsilon}_{2s}}{\psi} \quad (19a)$$

$$\psi = \theta \sin 2\alpha \quad (19b)$$

$$H = \frac{4\bar{\varepsilon}_2}{\gamma_{lt} \sin 2\alpha} \quad (19c)$$

$$t_d = \frac{1}{2(H+4)} \left[P_c \left(1 + \frac{H}{2} \right) - \sqrt{\left(1 + \frac{H}{2} \right)^2 P_c^2 - 4H(H+4)A_c} \right] \quad (19d)$$

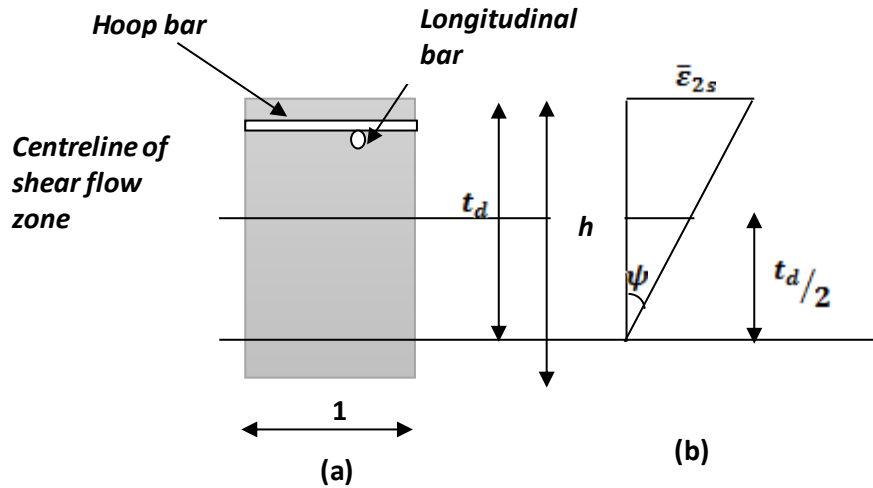


Fig.4.3.3 (a) Cross section of concrete strut Fig.4.3.3 (b) Strain distribution

4.3.3.2 Area (A_0) and perimeter (P_0) of a shear flow for a circular cross section

The expressions for the area (A_0) and the perimeter (P_0) of the shear flow are shown in Eqns. (19) and (20). The torque (T) and the twist (θ) in the member can be calculated from the expressions given in Eqns. (21) and (22).

$$A_0 = A_c - \frac{P_c t_d}{2} + \frac{\pi}{4} t_d^2 \quad (20)$$

$$P_0 = P_c - \pi t_d \quad (21)$$

$$T = 2A_0 t_d \tau_{lt} \quad (22)$$

$$\theta = \frac{P_0}{2A_0} \gamma_{lt} \quad (23)$$

4.3.3.3 Poisson's Effect:

Strain in a membrane element in any direction is a function of not only stress in that direction but also stress in the perpendicular direction. SMM for shear developed by Hsu and Zhu (2002) included this biaxial effect in terms of new parameter named as Hsu/Zhu ratio. This ratios are expressed as shown in the Eqns. (23) and (24). The ratio was modified by Jeng and Hsu (2009) to take strain gradient into account. The Hsu/Zhu ratio for torsion was taken as 0.8 times the ratio used for shear. Biaxial strains are related to uniaxial strains as shown in Eqns. (25) - (28).

$$\nu_{12} = 0.16 + 680\varepsilon_{sf} \quad \varepsilon_{sf} \leq \varepsilon_y \quad (24a)$$

$$\nu_{12} = 1.52 \quad \varepsilon_{sf} > \varepsilon_y \quad (24b)$$

$$\nu_{21} = 0 \quad (25)$$

$$\bar{\varepsilon}_1 = \frac{1}{1 - \nu_{12}\nu_{21}}\varepsilon_1 + \frac{\nu_{12}}{1 - \nu_{12}\nu_{21}}\varepsilon_2 \quad (26)$$

$$\bar{\varepsilon}_2 = \frac{\nu_{21}}{1 - \nu_{12}\nu_{21}}\varepsilon_1 + \frac{1}{1 - \nu_{12}\nu_{21}}\varepsilon_2 \quad (27)$$

$$\bar{\varepsilon}_l = \bar{\varepsilon}_1 \cos^2 \alpha + \bar{\varepsilon}_2 \sin^2 \alpha - \frac{\nu_{12}}{2} 2 \sin \alpha \cos \alpha \quad (28)$$

$$\bar{\varepsilon}_t = \bar{\varepsilon}_1 \sin^2 \alpha + \bar{\varepsilon}_2 \cos^2 \alpha + \frac{\nu_{12}}{2} 2 \sin \alpha \cos \alpha \quad (29)$$

As in the SMMT, the first two basic equilibrium equations Eq. (1) and Eq. (2) are summed and subtracted to obtain the following two equations, which are used as the convergence criteria for the solution procedure.

$$\rho_l f_l + \rho_t f_t + \rho_f f_f = (\sigma_l + \sigma_t) - (\sigma_{1c} + \sigma_{2c}) \quad (30)$$

$$\rho_l f_l - \rho_t f_t - \rho_f f_f = (\sigma_l - \sigma_t) - (\sigma_{1c} - \sigma_{2c}) \cos 2\alpha + 2\tau_{12c} \sin 2\alpha \quad (31)$$

4.3.4 Solution Algorithm for SMMT-FRP:

A strain controlled solution algorithm for SMMT-FRP which includes modified constitutive laws of concrete in compression and tension is shown in Fig.4.3.4. The solution algorithm is implemented in MATLAB.

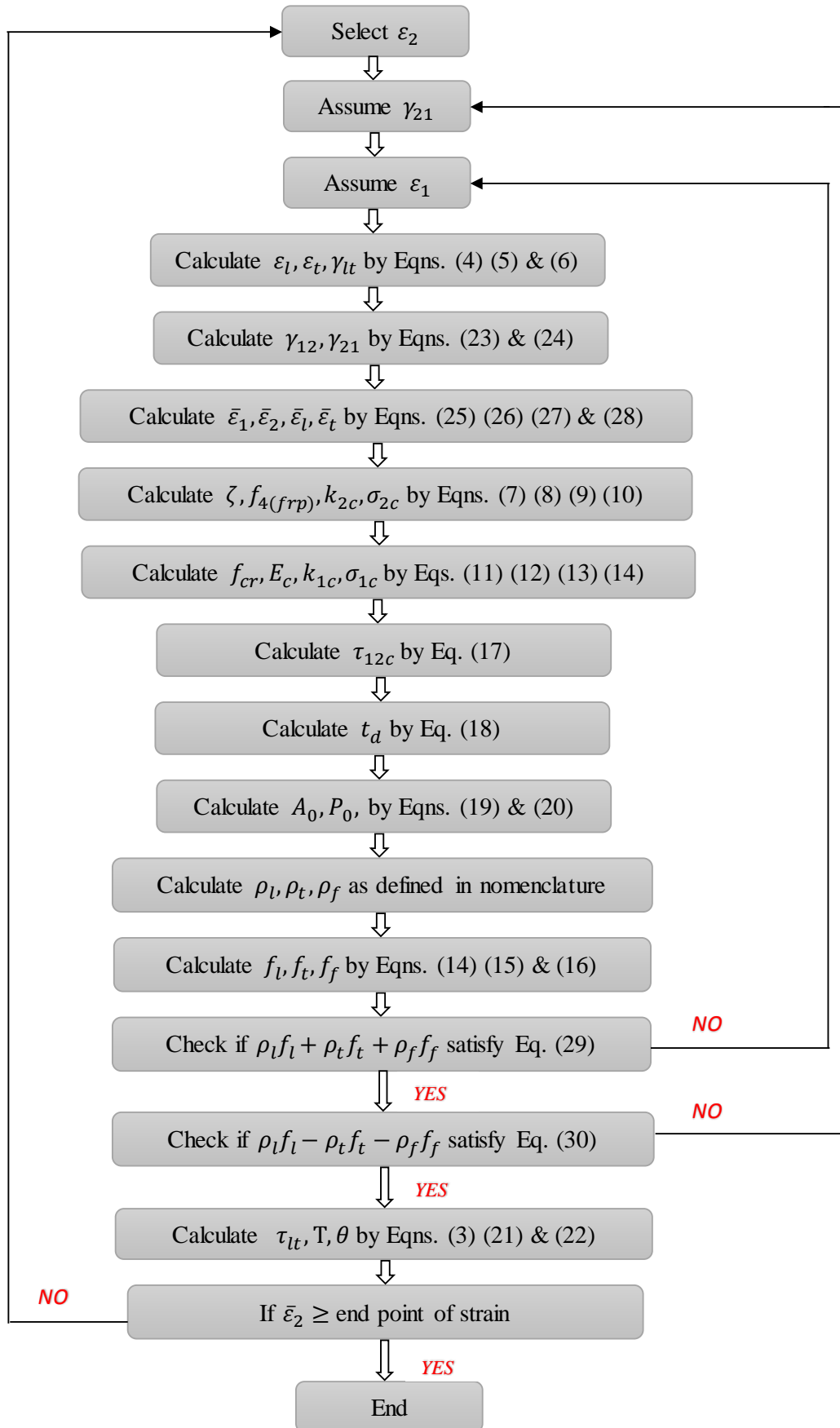


Fig. 4.3.4 Solution Algorithm of SMMT-FRP

4.3.5 NOMENCLATURE:

A_0	=	Area enclosed by the centreline of shear flow.
A_l	=	Total cross-sectional area of longitudinal steel bars.
A_t	=	Cross-sectional area of one transverse steel bar.
A_c	=	Cross-sectional area bounded by the outer perimeter of the concrete.
B	=	Variable as defined in the constitutive relationship of mild steel bar.
E_c	=	Elastic modulus of concrete
E_s	=	Elastic modulus of the steel bars
E_{frp}	=	Modulus of elasticity of FRP sheets.
f_c'	=	Cylinder compressive strength of concrete
f_{cr}	=	Cracking stress of concrete
f_l	=	Smearred (average) steel stress in the longitudinal direction.
f_t	=	Smearred (average) steel stress in the transverse direction.
f_s	=	Smearred (average) stress of steel bars
f_y	=	Yield stress of bare steel bars.
k_{1c}	=	Ratio of average tensile stress of the peak tensile stress in the concrete struts.
k_{2c}	=	Ratio of the average compressive stress to the peak compressive stress in the concrete struts.
nft	=	Number of layers of FRP sheets.
P_0	=	Perimeter of the centreline of shear flow.
P_c	=	Perimeter of the outer concrete cross section.
q	=	Shear flow
H	=	Variable as defined to calculate the thickness of the shear flow zone.
s	=	Spacing of transverse hoop bars.
T	=	Torque
w_f	=	Width of FRP sheets.
t_d	=	Thickness of shear flow zone.
t_{frp}	=	Thickness of FRP sheets.

- w = Out-of-plane displacement in the direction normal to the membrane element.
- α = Fixed angle, angle of applied principal compressive stress (2-axis) with respect to longitudinal steel bars.
- β = Deviation angle
- ε_0 = Concrete cylinder strain corresponding to peak cylinder strength, f'_c
- $\varepsilon_1, \varepsilon_2$ = Smear (average) biaxial strain in the 1-direction and the 2-direction, respectively.
- $\bar{\varepsilon}_1, \bar{\varepsilon}_2$ = Smear (average) uniaxial strain in the 1-direction and the 2-direction, respectively.
- $\varepsilon_l, \varepsilon_t$ = Smear (average) biaxial strain in the l -direction and the t -direction, respectively.
- $\bar{\varepsilon}_l, \bar{\varepsilon}_t$ = Smear (average) uniaxial strain in the l -direction and the t -direction, respectively.
- ε_{cr} = Cracking strain of concrete.
- ε_y = Yield strain of steel bars.
- $\bar{\varepsilon}_{1s}, \bar{\varepsilon}_{2s}$ = Uniaxial surface strain in the 1-direction and the 2-direction, respectively
- $\bar{\varepsilon}_s$ = Smear (average) uniaxial strain of the steel bars.
- γ_{21} = Smear (average) shear strain in the 2-1 coordinate.
- γ_{lt} = Smear (average) shear strain in the lt coordinate of the steel bars.
- σ_{1c} = Smear (average) normal stresses of concrete in the 1-direction.
- σ_{2c} = Smear (average) normal stresses of concrete in the 2-direction.
- σ_l, σ_t = Applied normal stresses in the l -direction and the t -direction of the steel bars respectively.
- τ_{12c} = Smear (average) shear stress of concrete in 2-1 coordinate.
- τ_{lt} = Applied shear stresses in the lt coordinate of the steel bars.
- ρ_l, ρ_t = Longitudinal and transverse steel ratios respectively.
- $\rho_l = A_l/P_0t_d$; $\rho_t = A_t/st_d$
- v_{12}, v_{21} = Hsu/Zhu ratios.

- θ = Angle of twist per unit length.
- ψ = Curvature of the concrete struts.
- ζ = Softened coefficient of concrete in compression.

CHAPTER-5

RESULTS & DISCUSSIONS

RESULTS AND DISCUSSION

PART-I

5.1 VALIDATION OF THE DEVELOPED MODEL (F.E.A):

The overall torque-twist behaviour captured from the developed FE model has shown a good agreement with the experimental results. It is shown in Fig.5.1 (a) and Fig.5.1 (b) for circular and square columns respectively. FE model overestimates the ultimate torsional capacity, only to a limited extent. The unstable behaviour of the developed FE model for square column in the post peak region and the overestimation of torsional capacity can be attributed to size effect, material and geometric imperfections (Claeson and Johansson 1999) which are not considered in the FE model. The torsional stiffness predicted by the finite element model was close to the measured values, particularly in the pre-cracking and post-peak region. It shows that the developed model is equally effective in predicting the local and the global behaviour of reinforced concrete members with a considerable amount of accuracy. The damage distribution is also validated with experimental result for the circular column under pure torsion as shown in Fig.5.1 (c).

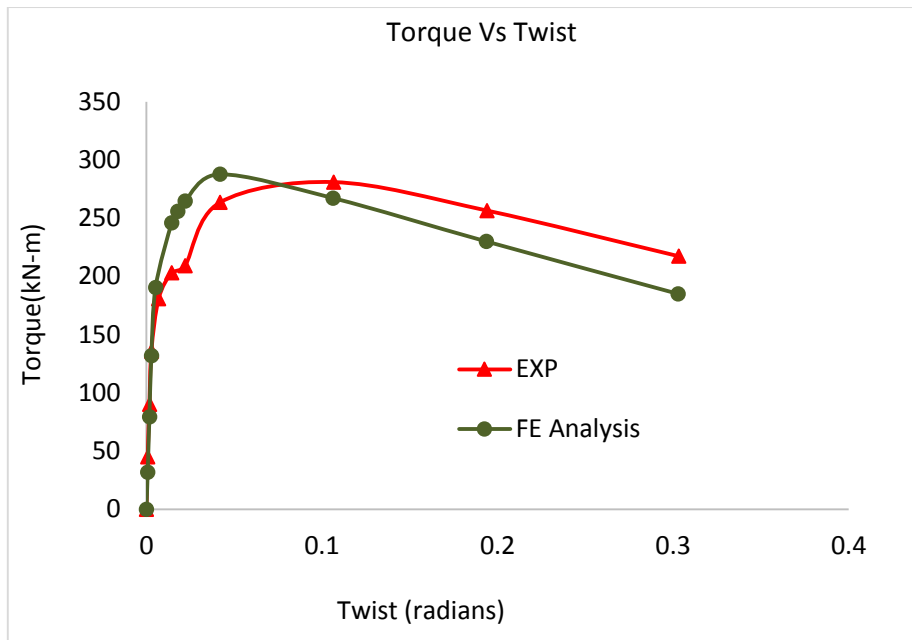


Fig.5.1 (a) Over-all torque-twist behaviour of circular column

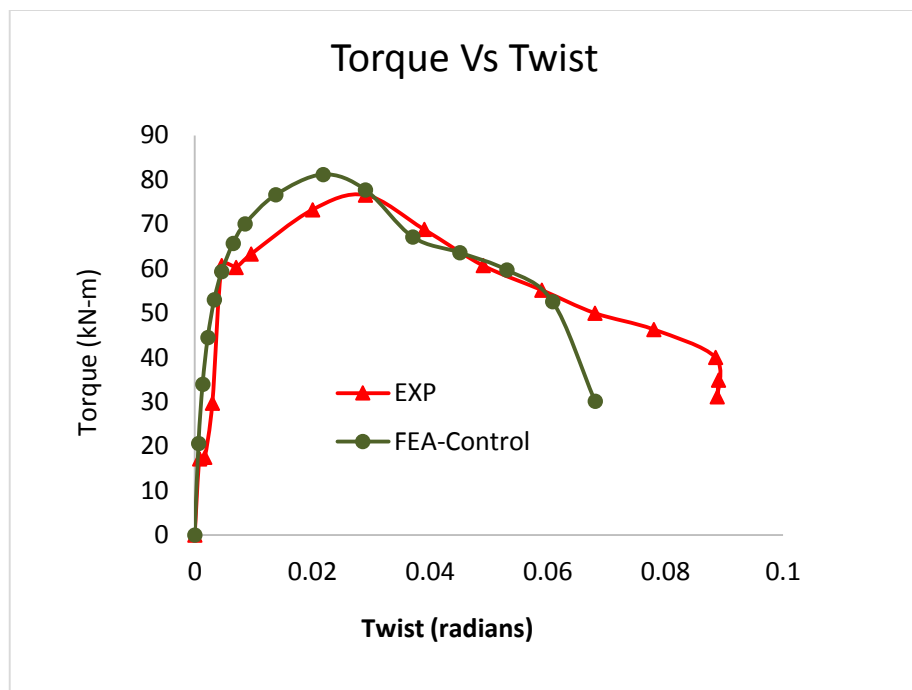


Fig.5.1 (b) Over-all torque-twist behaviour of a square column


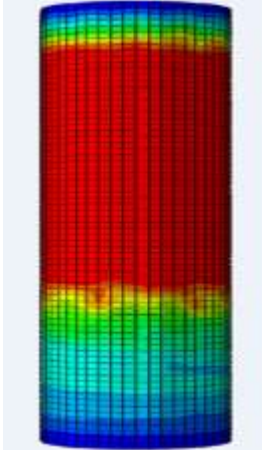
<i>Specimen Id</i>	<i>Experimental</i>	<i>FE Analysis</i>	<i>FE Analysis</i>
		<i>Contour</i>	<i>Legend</i>
H/D(6)- T/M(∞)-0.73% Circular column			<p>DAMAGET (Avg: 75%)</p> <ul style="list-style-type: none"> +9.973e-01 +9.165e-01 +8.357e-01 +7.549e-01 +6.741e-01 +5.932e-01 +5.124e-01 +4.316e-01 +3.508e-01 +2.700e-01 +1.892e-01 +1.084e-01 +2.760e-02

Fig.5.1 (c) Damage distribution of circular column under torsion

5.2 EFFECT OF STRENGTHENING THE COLUMNS WITH FRP:

As the developed FE models resulted in good agreement with experimental, here an assumption is made that the developed FE models when regenerated and analysed by strengthening with FRP gives the appropriate behaviour in all aspects.

The experimental validated FE models are regenerated by externally wrapping with FRP around the column at the middle one-third height of the column. The overall torque-twist behaviour is represented in Fig.5.2 (a) and Fig.5.2 (b) for square and circular columns respectively. The ultimate increase in torsional capacity and post peak behaviour of the circular column strengthened with FRP is higher than the square column strengthened with FRP. When the damage distributions are compared, the square column exhibited more localized damage whereas in the circular columns

damage was distributed all over the length. This implies that cross section of column has influence on damage distribution. The damage distributions are represented in Fig.5.2 (c).

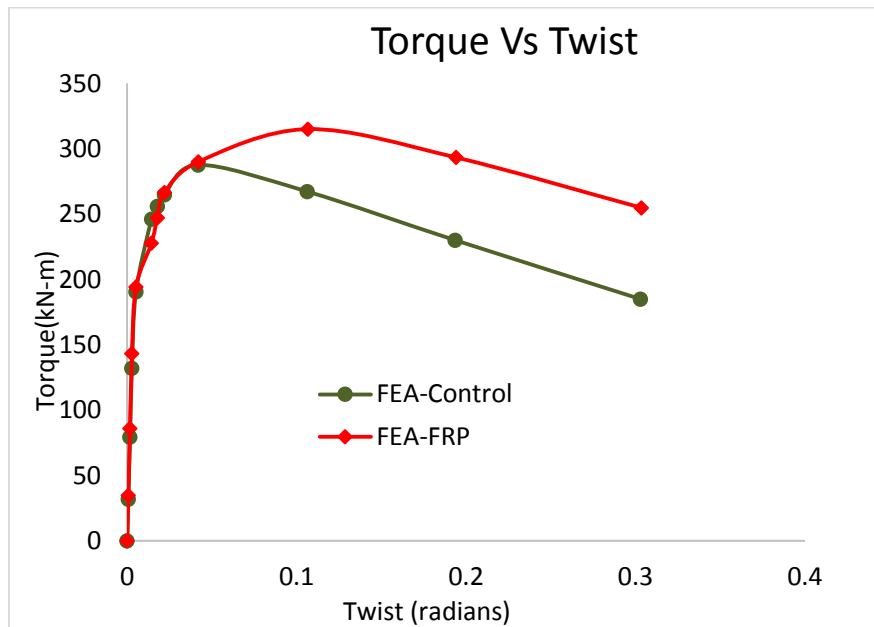


Fig.5.2 (a) Over-all torque-twist behaviour of circular column strengthened with FRP

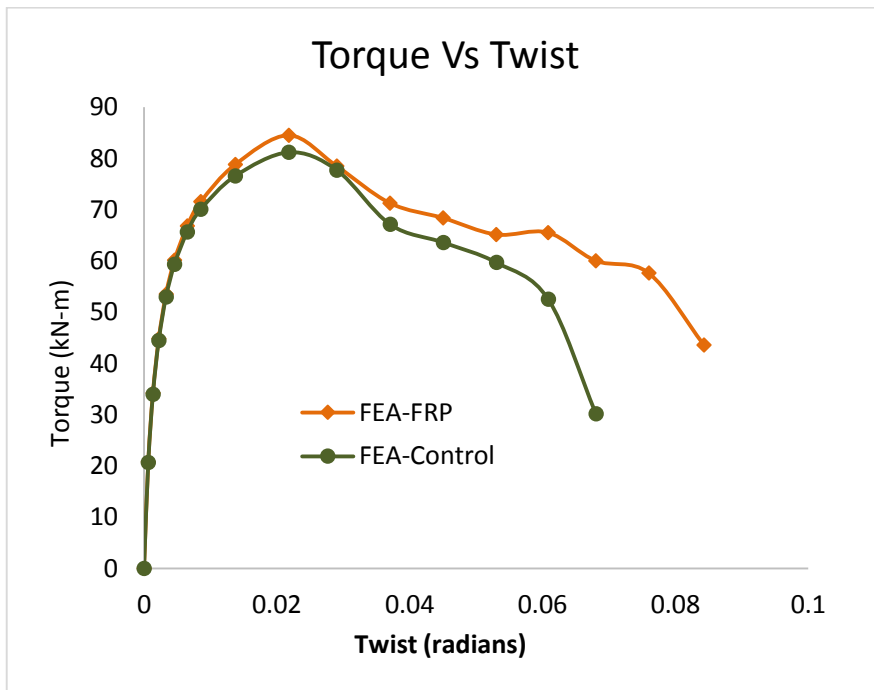


Fig.5.2 (b) Over-all torque-twist behaviour of square column strengthened with FRP

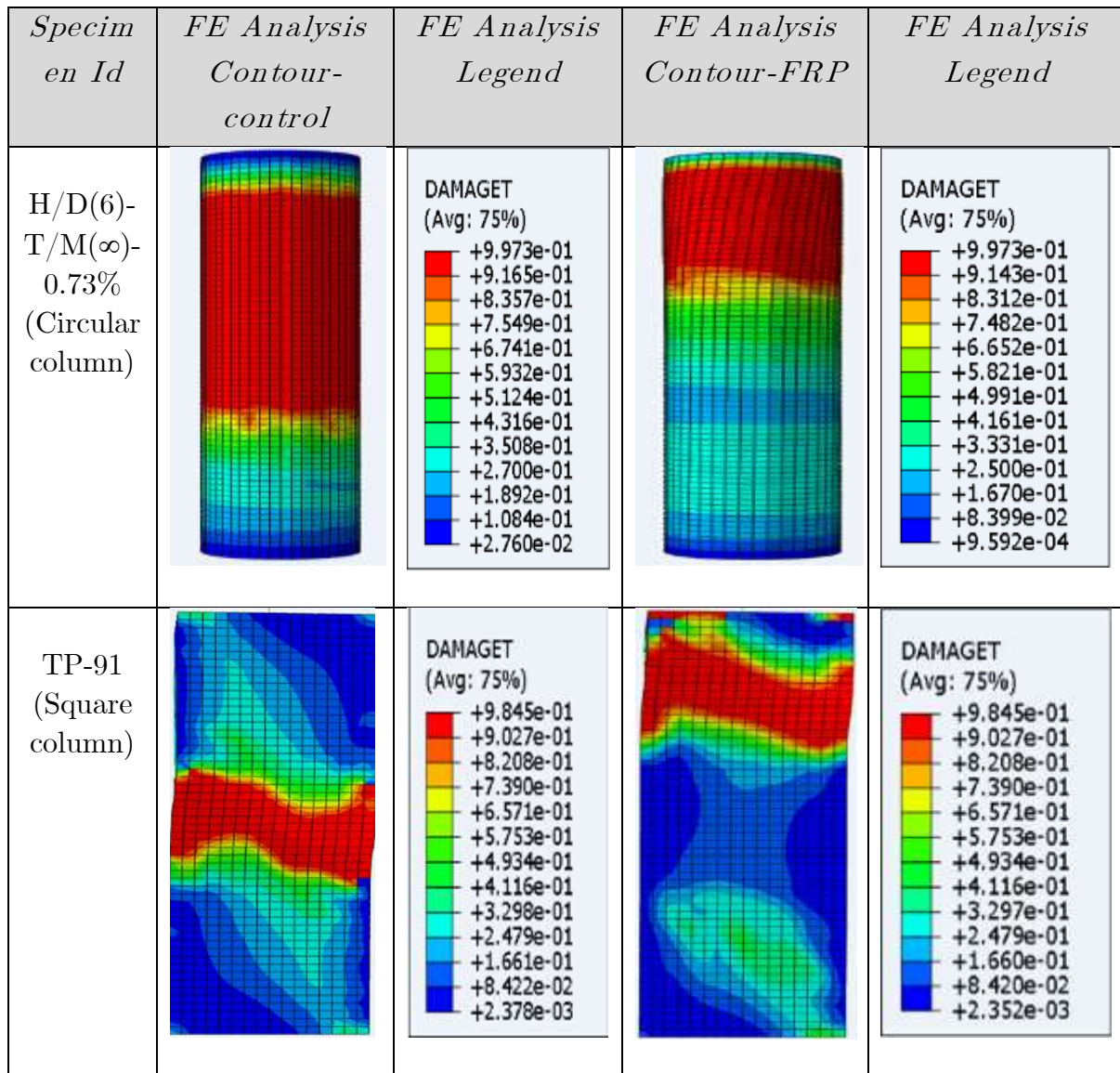


Fig.5.2 (c) Damage distribution of columns strengthened with and without FRP under torsion

PART-II

5.3 VALIDATION OF THE DEVELOPED MODEL (MATLAB):

The overall torque-twist behaviour predicted using SMMT theory in MATLAB has shown good agreement with the experimental and Finite Element result. The Fig. 5.3 shows the validation of Torque-Twist behaviour of a reinforced concrete circular column subjected to torsion. Initial stiffness and post peak behaviour are having a good match. The details of the specimen used are mentioned in Table-I. The cross-section of the circular column is shown in Fig.3.1 (a).

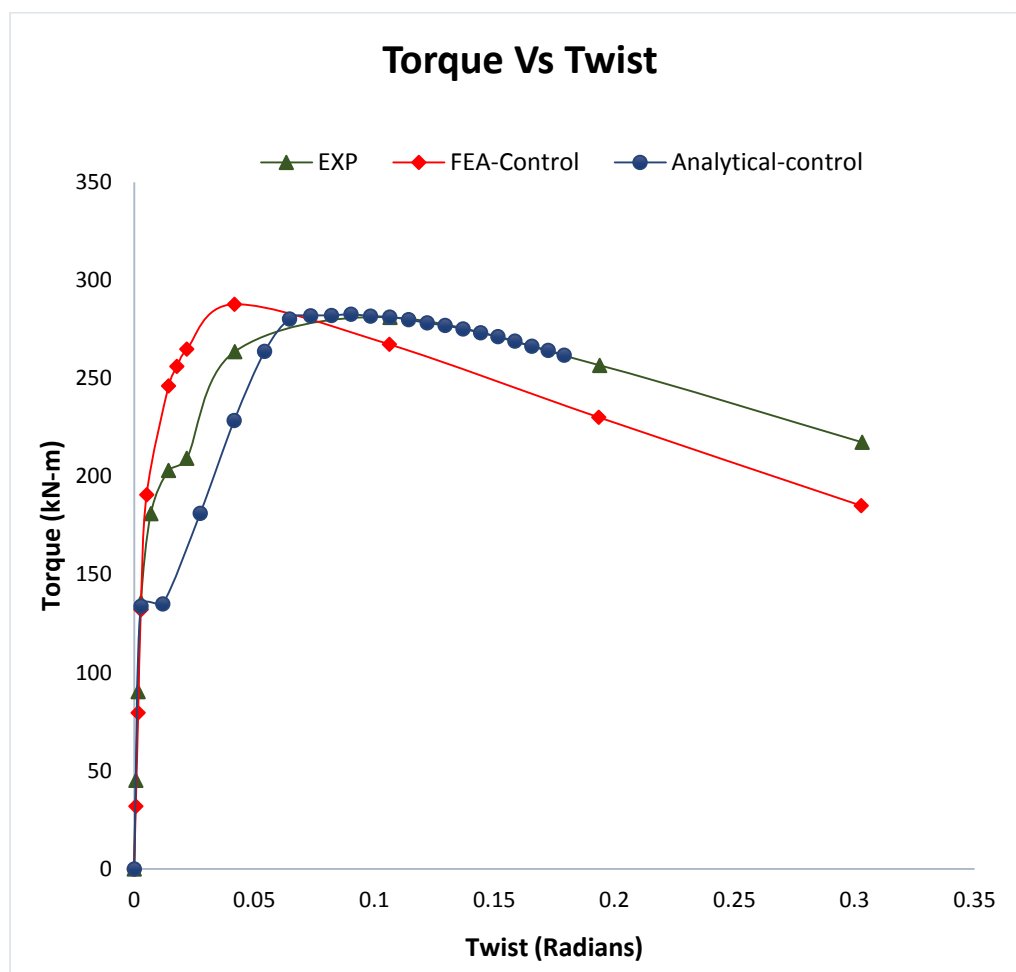


Fig.5.3 Overall Torque-Twist behaviour of circular column

5.4 EFFECT OF STRENGTHENING THE COLUMNS WITH FRP:

As the developed SMMT code in MATLAB gave a result that has good agreement with the experimental specimen, an assumption has been made that the same code modified with equations that include FRP properties will also give an approximately reliable results for the R.C circular columns strengthened with FRP, which don't have an experimental data for validation.

Analysis has been carried out by externally wrapping the FRP at the middle one-third height of the column. Fibre direction is perpendicular to the longitudinal axis of the column. The overall torque-twist behaviour is represented in Fig.5.4.

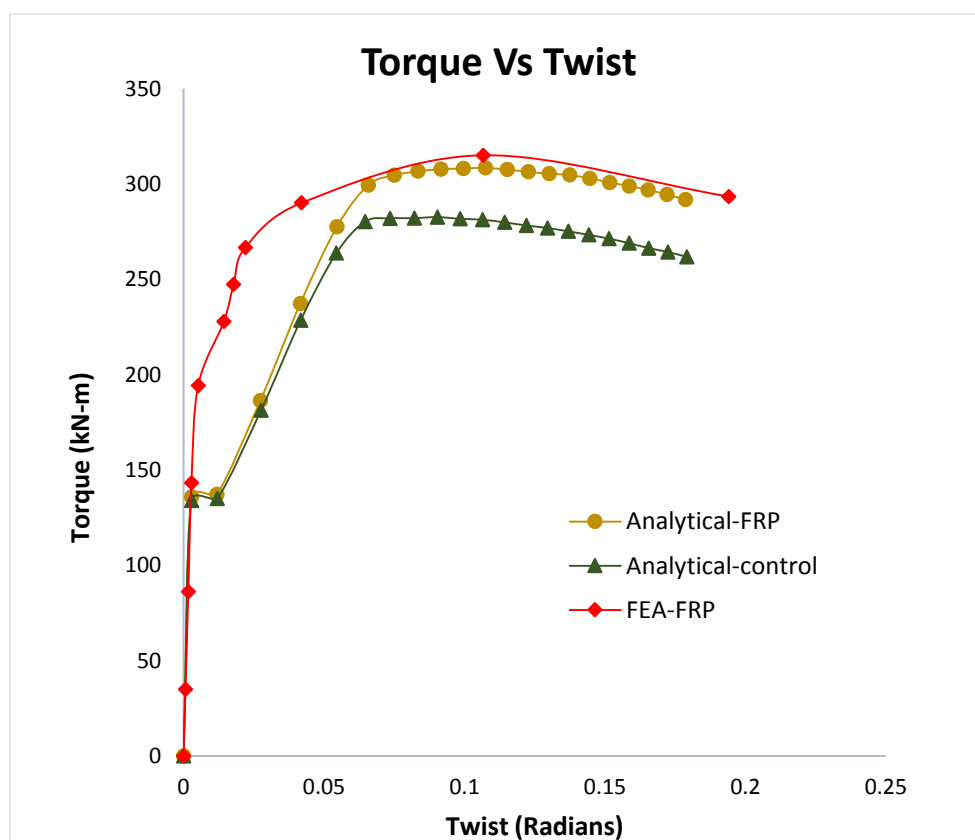


Fig.5.4 Torque-twist behaviour of columns strengthened with and without FRP

5.5 PARAMETRIC STUDY:

Parametric study has been carried on by varying the parameters like thickness of FRP sheets, number of layers of FRP sheets, alignment of FRP sheets and increasing the axial load.

5.5.1 EFFECT OF THICKNESS OF FRP SHEET:

The overall torque-twist behavior predicted by varying the thickness of FRP sheet from 1mm to 3mm is shown in Fig.5.5.1. The predictions implies that even if the thickness of the FRP is continuously increased there is no much difference in between the post-crack and pre-peak behavior. But there is a significant increase in post-peak behavior which can be observed in the terms of increased peak torsional moment which shows the effect of increasing the thickness of FRP sheets.

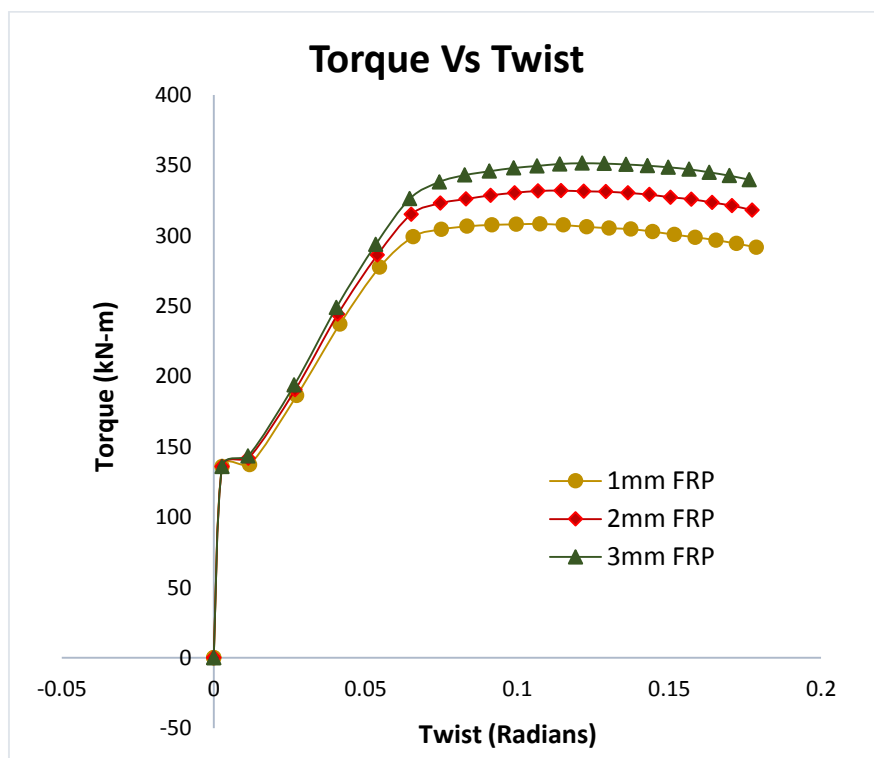


Fig.5.5.1 Torque-Twist behaviour of circular column by varying FRP thickness

5.5.2 EFFECT OF MULTIPLE LAYERS OF FRP SHEETS:

The overall torque-twist behavior predicted by varying the number of layers of FRP of constant thickness is shown in Fig.5.5.2 (a) and 5.5.2(b). It is observed that peak torsional moment and post peak behavior has been significantly increased by increasing the layers of FRP sheets. Here the bond characteristics between multiple layers of FRP sheets is assumed to behave like a perfect bond. The torque-twist behavior of reinforced concrete circular column externally wrapped with 2mm FRP sheet is approximately similar to the behavior of reinforced concrete circular column externally wrapped with 2layers of 1mm FRP sheets. The similar observation is made for the cases with 3mm FRP sheet and 3 layer of 1mm FRP sheet. This behaviour may change if different bond characteristics are considered, which is a scope for future study.

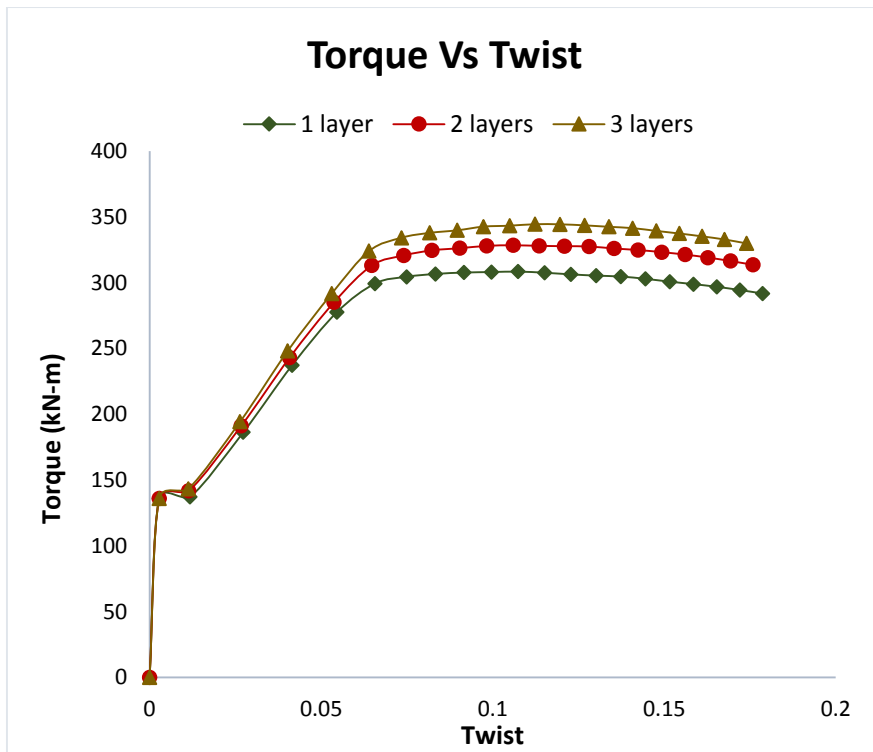


Fig.5.5.2 (a) Torque-twist behaviour of columns with 1mm FRP by varying layers

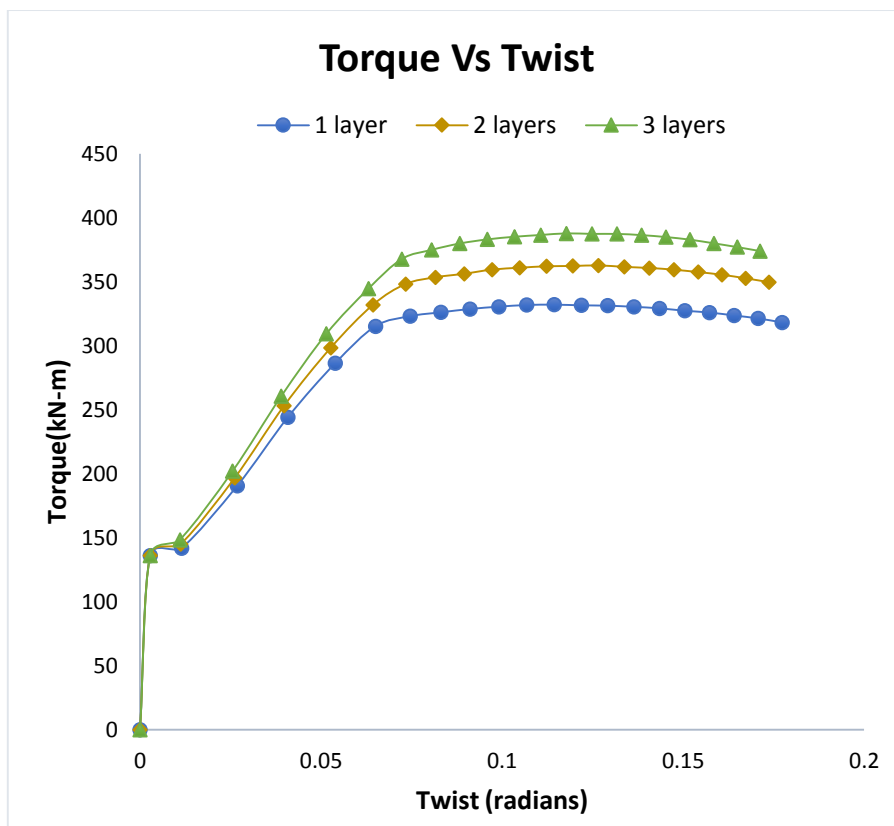


Fig.5.5.2 (b) Torque-twist behaviour of columns with 2mm FRP by varying layers

5.5.3 EFFECT OF FRP SHEET ALIGNMENT:

FRP sheets are aligned at various angles i.e., 0° , 30° , 45° , 60° and 90° with respect to the direction of transverse reinforcement and overall torque-twist behavior is predicted. For the given circular section the amount of longitudinal and transverse reinforcement are 2.1% and 0.73% respectively which infers that crack tends to propagate more in the direction of transverse reinforcement. Here the predictions developed for various alignments of FRP with respect to transverse direction (Fig.5.5.3) shows that FRP is more efficient in resisting cracks and increasing peak torsional moment when it is aligned at an angle of 60° .

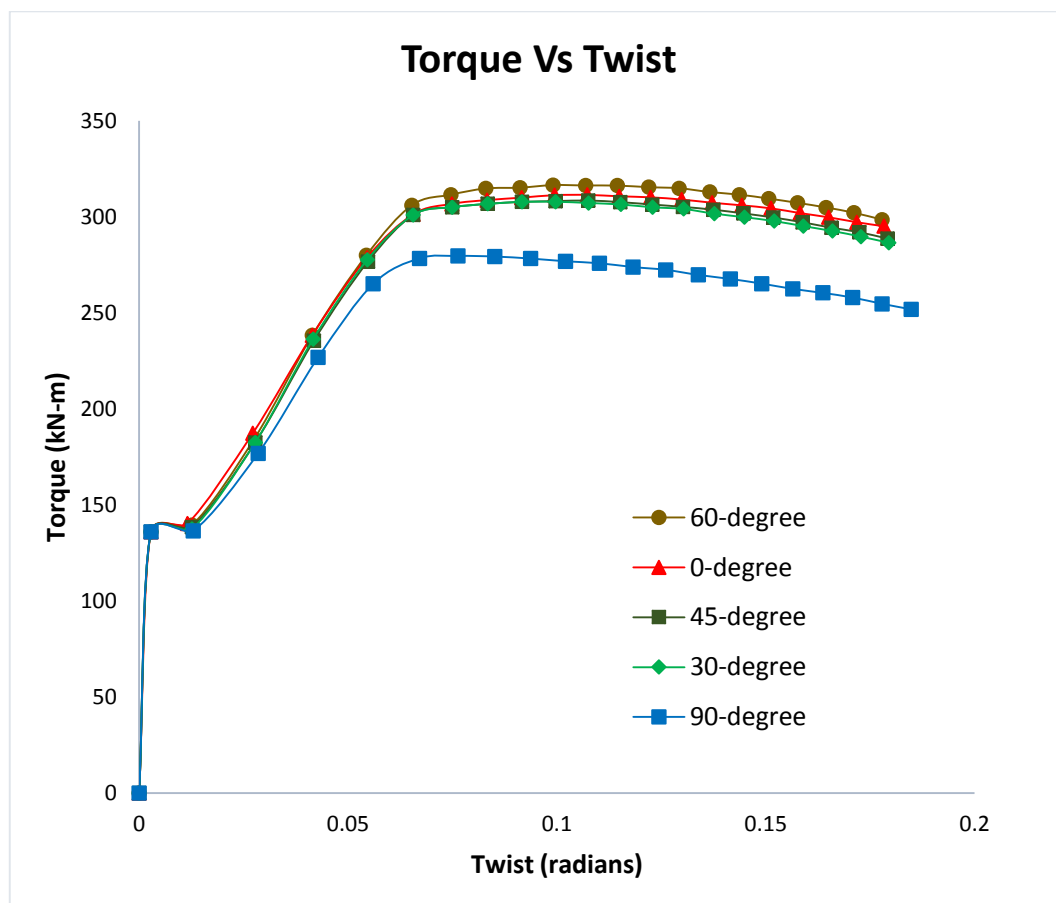


Fig.5.5.3 Torque-Twist behaviour of column at various alignment of FRP direction

5.5.4 EFFECT OF AXIAL COMPRESSION:

5.5.4.1 UNSTRENGTHENED COLUMNS:

The effect of axial compression is studied by predicting the torque-twist behavior of the reinforced concrete circular column which is subjected to axial compression in addition to torsion. The presence of axial compressive load delays in the tensile stresses that are arising from torsion and thus delaying the cracking of concrete under diagonal tension. The cracking torsional capacity of RC members increases significantly in the presence of axial compressive load. This increase in torsional capacity reaches maximum value at the level of axial compression that totally restrain the column elongation due to torsion. As the axial compression dominates, the failure will be sudden in the form of crushing of concrete. It can be observed from Fig.5.5.4 (a) that addition of axial compression to torsion adds up on to increase in torsional moment up to certain extent and further more increase in axial load starts decreasing the torsional capacity of the column with the change in failure mode.

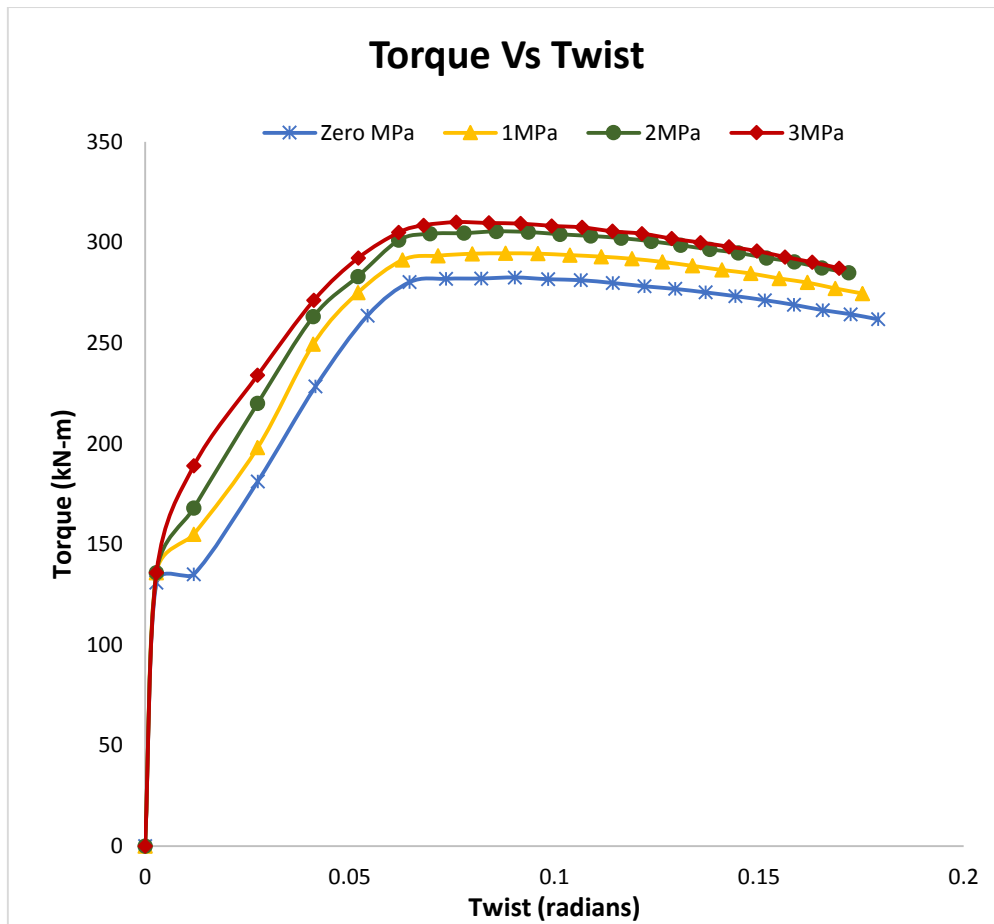


Fig.5.5.4 (a) Torque-twist behaviour of column under torsion and various axial loads

5.5.4.2 FRP STRENGTHENED COLUMNS:

FRP provides passive confinement to the compression member, remaining unstressed until dilation and cracking of the wrapped compression member occur. There is an enhancement of peak torsional capacity and post peak behaviour for the FRP strengthened columns when compared with unstrengthened columns for the same amount of axial compression. This significance of FRP contribution can be clearly noticed in Fig.5.5.4 (c).

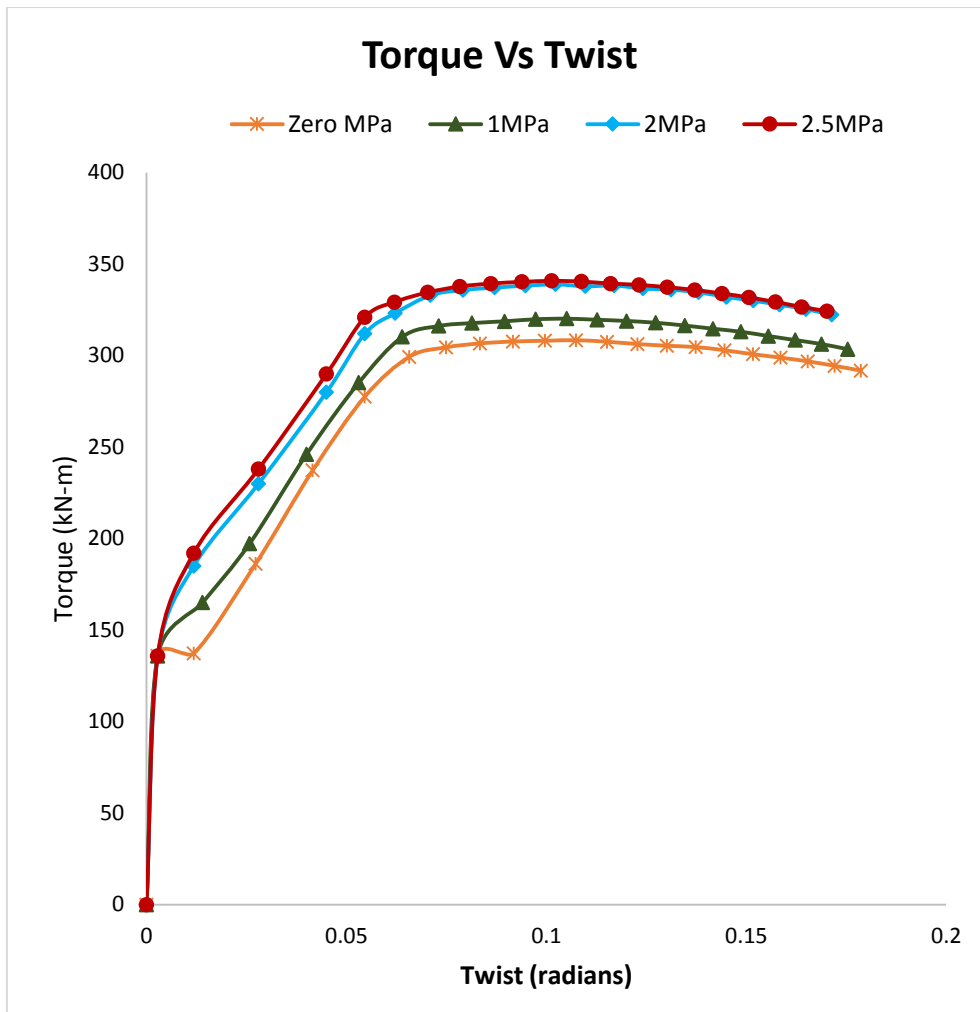


Fig.5.5.4 (b) Torque-twist behaviour of FRP columns under torsion and various axial load

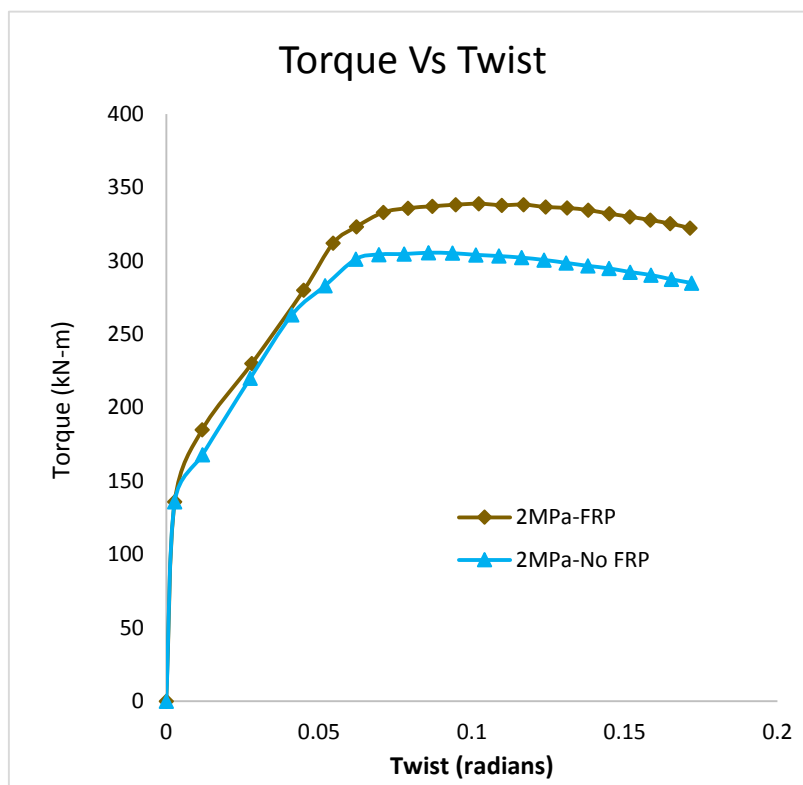
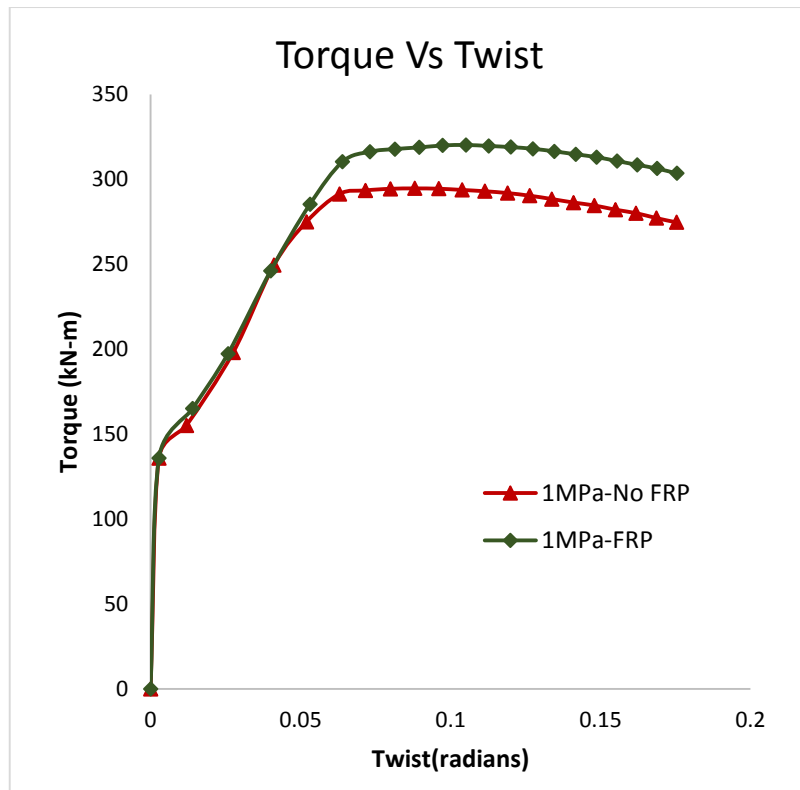


Fig.5.5.4 (c) Torque-twist behaviour of columns with and without FRP for same axial load

5.5.5 TORSION-AXIAL LOAD INTERACTION DIAGRAM:

A failure interaction curve between axial compression and torsional moment was developed for both the columns strengthened with and without FRP as shown in the Fig. 5.5.5. (b). The curve started at the point of pure torsion and is extended up to the point of pure axial compression. At low levels of axial compression, the torsional capacity of a section is enhanced as in the case of axial compression and bending interaction diagram. The interaction curve encounters a kink point after which the failure mode changes to crushing of concrete under diagonal compression. This limits the enhancement of torsional strength with increase in axial compressive load which can be clearly noticed in the Fig. 5.5.5(b).

The point of pure axial compression for both the cases is manually calculated. For the case of unstrengthened column, axial compression capacity is calculated as per the norms mentioned in IS-456.

$$P_u = (0.4f_{ck}A_c) + (0.67f_yA_{sc})$$

Where

P_u = Axial compression capacity (N)

f_{ck} = Compressive strength of concrete (MPa)

A_c = Area of concrete (mm²)

A_{sc} = Area of longitudinal steel (mm²)

f_y = Yield stress of longitudinal steel (MPa)

For the case of column strengthened with FRP, the confined compressive capacity of a column is calculated as per ACI.440.2R-08. Confining a concrete member is accomplished by orienting the fibers transverse to the longitudinal axis of the member. In this orientation, the transverse or hoop fibres are similar to conventional spiral or tie reinforcing steel. Any contribution of longitudinally aligned fibers to the axial compression strength of a concrete member should be neglected. The stress-strain model for FRP confined concrete is shown in Fig. 5.5.5(a) and is computed by the following equations:

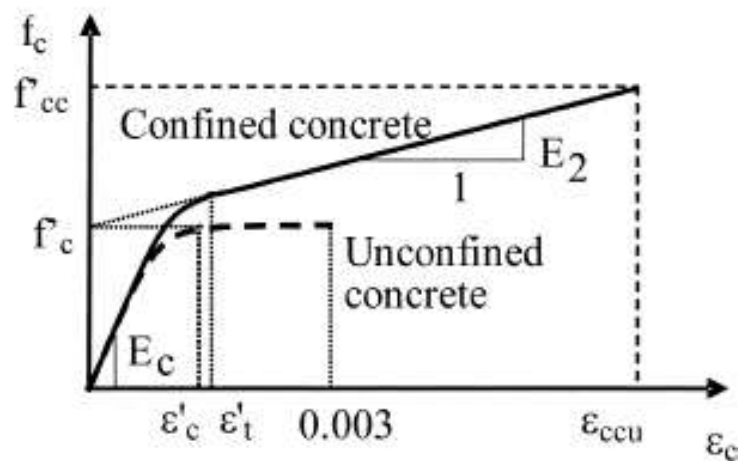


Fig. 5.5.5(a) Stress strain curve for unconfined and FRP confined concrete

$$f_c = \begin{cases} E_c \varepsilon_c - \frac{(E_c - E_2)^2}{4f'_c} \varepsilon_c^2 & 0 \leq \varepsilon_c \leq \varepsilon'_t \\ f'_c + E_2 \varepsilon_c & \varepsilon'_t \leq \varepsilon_c \leq \varepsilon_{ccu} \end{cases}$$

$$E_2 = \frac{f'_{cc} - f'_c}{\varepsilon_{ccu}}$$

$$\varepsilon'_t = \frac{2f'_c}{E_c - E_2}$$

The maximum confined compressive strength of concrete (f_{cc}') is calculated in terms of maximum confinement pressure (f_l) as mentioned below.

$$f_{cc}' = f_c' \left(1 + \psi_f 3.3 k_a \frac{f_l}{f_c'} \right)$$

ψ_f is the additional reduction factor and is equal to 0.95. k_a and k_b are the shape factors and for circular sections its value is one.

$$f_l = \frac{2E_f n t_f \varepsilon_{fe}}{D}$$

Where,

E_f - Modulus of Elasticity of FRP

n - Number of layers of FRP

t_f - Thickness of FRP sheets

ε_{fe} - Effective strain level in the FRP at failure.

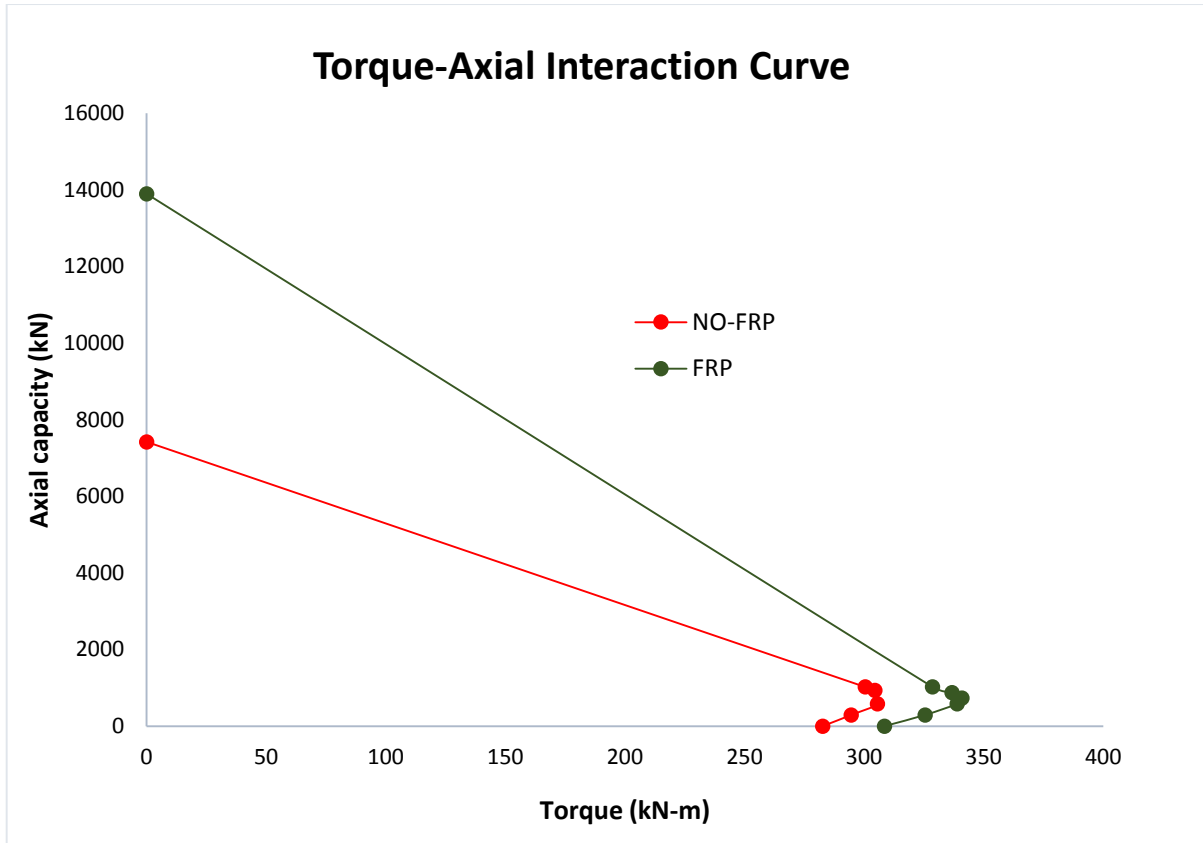


Fig.5.5.5 (b) Axial compression – Torsional moment Interaction diagram

$$\varepsilon_{fe} = k_{\varepsilon} \varepsilon_{fu}$$

k_{ε} is the FRP efficiency factor which accounts for the premature failure of FRP system.

The maximum compressive strain in the confined concrete (ε_{ccu}) given in the below equation should be limited to 0.01 as per code to prevent the excessive cracking and the resulting loss of concrete integrity.

$$\varepsilon_{ccu} = \varepsilon_c' \left(1.50 + 12k_b \frac{f_l}{f_c'} \left(\frac{\varepsilon_{fe}}{\varepsilon_c'} \right)^{0.45} \right)$$

CHAPTER-6

CONCLUSIONS & SCOPE FOR FUTURE STUDY

CHAPTER – 6

6.1 CONCLUSIONS:

The analytical model developed to predict the torsional behaviour of FRP strengthened R.C members considering the effect of FRP confinement and cross sectional shape has resulted in following conclusions which are summarized below:

- ✓ Analytical and F.E models developed for unstrengthened columns have predicted the torsional behaviour of columns with fair degree of accuracy.
- ✓ Effect of cross section plays a major role in the distribution of damage in columns.
- ✓ FRP composites has shown increase in the ultimate strength and post cracking stiffness of the columns under torsion.
- ✓ The predicted torsional behaviour of FRP composites at various angles with respect to transverse direction has shown that FRP is more effective when it is aligned at an angle of 60 degree.
- ✓ The torsion- axial interaction developed is similar to bending- axial interaction diagram.

- ✓ FRP wrapped columns axial-torsion behaviour shows the significant contribution of FRP in terms of peak torsional capacity and post peak behaviour.

6.2 SCOPE FOR FUTURE STUDY:

- ✓ Non-linear FE analysis can also be carried for all the parametric studies like varying the thickness, number of layers and alignment of FRP sheets that has been done by making use of SMMT-FRP theory in MATLAB.
- ✓ Till now there exists no experimental test data for the above study. Conducting experiments on circular columns that are externally wrapped with FRP subjected to torsion is a good scope of future study.

6.3 REFERENCES:

- Abaqus Analysis User's Manual 6.11. Dassault Systèmes Simulia Corporation, Providence, RI, USA.
- Ameli, M, Ronagh, H.R, Dux, P.F (2007). “Behavior of FRP strengthened Reinforced Concrete Beams under Torsion.” *Journal of Bridge Engineering*, ASCE library, DOI- 10.1061/ASCE-1090-0268-2007
- Anand, G. G., Mondal, T. G., Prakash, S. S. (2015). “Improved Softened Membrane Model for Reinforced Concrete Circular Bridge Columns under Torsional Loading”. *Journal of Bridge Engineerig*, ASCE library, DOI: 10.1061/(ASCE)BE.1943-5592.0000907.
- Belarbi, A., and Hsu, T. T. (1994). “Constitutive laws of concrete in tension and reinforcing bars stiffened by concrete.” *ACI structural Journal*, 91 (4) 465-474.
- Chalioris, C. E. (2007). “Analytical model for the torsional behaviour of reinforced concrete beams retrofitted with FRP materials”. *Engineering Structures*, 29(12), 3263-3276.

- Claeson, C. and Johansson, M. (1999). "Finite element analysis of confined concrete columns." *Proceedings of the fifth international symposium on utilization of high-strength/high-performance concrete*, Sandefjord, Norway.
- Delso, J. M., Stavridis, A., and Shing, B. (2011). "Modeling the Bond-Slip Behavior of Confined Large Diameter Reinforcing Bars." *III ECCOMAS Thematic Conference on Computational Methods in Structural Dynamics and Earthquake Engineering COMPDYN*, Corfu, Greece.
- Floros, D., and Ingason, O. A. (2013). "Modeling and Simulation of Reinforced Concrete Beams: Coupled Analysis of Imperfectly Bonded Reinforcement in Fracturing Concrete." Master's Thesis 2013:42, Department of Applied Mechanics: Division of Solid Mechaics, Goteborg, Sweden.
- Hadi, M.N.S (2006). "Behavior of FRP wrapped normal strength concrete columns under eccentric loading." *Engineering Structures Journal*, Elsevier,72,pp 503-511.
- Hsu, T. T. C. (1968a). "Torsion of Structural Concrete - Behavior of Reinforced Concrete Rectangular Members." *Torsion of Structural Concrete, SP-18*, American Concrete Institute, Detroit, MI.
- Hurtado, G. (2009). "Effect of Torsion on the Flexural Ductility of Reinforced Concrete Bridge Columns." Ph.D. Thesis, Department of Civil and Environmental Engineering, University of California, Berkeley.
- Jankowiak, T., and Lodygowski T. (2005). "Identification of Parameters of Concrete Damage Plasticity Constitutive Model." *Foundations of Civil and Environmental Engineering*, No. 6.
- Jeng, C. H., and Hsu, T. T. (2009). "A softened membrane model for torsion in reinforced concrete members." *Engineering Structures*, 31(9), 1944-1954.
- Mitchell, D. and Collins, M. P. (1974). "Diagonal Compression Field Theory - A Rational Model for Structural Concrete in Pure Torsion." *Journal of the American Concrete Institute*, 71, pp. 396-408.
- Mondal, T. G., and Prakash, S. S. (2015). "Nonlinear Finite-Element Analysis of RC Bridge Columns under Torsion with and without Axial Compression." *Journal of Bridge Engineering, ASCE library*, 04015037.
- Mondal, T. G., & Prakash, S. S. (2015). "Effect of tension stiffening on the behavior of reinforced concrete circular columns under torsion". *Engineering Structures*, 92, 186-195.
- Panchacharam, S and Belarbi, A "Torsional Behavior of Reinforced Concrete Beams Strengthened with FRP Composites," First FIB Congress, Osaka, Japan, October-2002

- Prakash, S. S. (2009). "Seismic Behavior of RC Circular Columns under Combined Loading Including Torsion." Department of Civil Engineering, Missouri University of Science and Technology, Missouri, USA.
- Rabbat, B. G., and Russell, H. G. (1985). "Friction Coefficient of Steel on Concrete or Grout." *Journal of Structural Engineering*, ASCE 111(3): 505-515.
- Rahal, K. N., and Collins, M. P. (1996). "Simple Model for Predicting Torsional Strength of Reinforced and Prestressed Concrete Sections." *ACI Structural Journal*, 93, 658-666.
- Rutledge, S.T., Kowalsky, M.J., Seracino, R., Nau, J.M. (2012). "Repair of Damaged Circular Reinforced Concrete Columns by Plastic Hinge Relocation." 15WCEE, LISBOA 2012, North Carolina State University, USA.
- Suman Dhara (2015)." Behavior of Precast Prestressed Hollow Core Slabs with and without FRP Strengthening." Department of Civil Engineering, Indian Institute of Technology, Hyderabad, India.
- Tirasit, P., and Kawashima, K. (2007a). "Seismic performance of square reinforced concrete columns under combined cyclic flexural and torsional loadings." *Journal of Earthquake Engineering*, 11, 425-452.
- Tirasit, P., and Kawashima, K. (2007b). "Effect of nonlinear torsion on the performance of skewed bridge piers." *Journal of Earthquake Engineering*, 12, 980-998.
- Vecchio, F. J., and Collins, M. P. (1986). "The Modified Compression-Field Theory for Reinforced Concrete Elements Subjected to Shear." *Journal of the American Concrete Institute*, 83, 219-231.
- Wang, J. (2006). "Constitutive relationships of prestressed concrete membrane elements." Ph.D. thesis, Dept. of Civil and Environmental Engineering, Univ. of Houston, Houston.
- Zhang, L. X. (1995). "Constitutive laws of reinforced elements with high strength concrete." Ph.D. thesis, Dept. of Civil and Environmental Engineering, Univ. of Houston, Houston.
- Zhu, R. R., and Hsu, T. T. (2002). "Poisson effect in reinforced concrete membrane elements." *ACI Structural Journal*, 99 (5), 631-640.